MASTER THESIS

Aerodynamic simulation and design of the undertray for the TU-WIEN Formula SAE race car

Executed at the Institute of Fluid Mechanics and Heat Transfer (E322) of

Vienna University of Technology

Supervised by

Ao. Prof. Dr. Herbert Steinrück

of

David Pérez Pons

Matriculation 1428085

Vienna, July 2015

ACKNOWLEDGEMENTS

I want to thank Ao. Prof. Dr. Herbert Steinrück for all of the support and advice he gave me for my thesis and all the people that have helped me at some points during the development of it. I would also like to thank TUW Racing Team for including me as a member of their race team in order to develop the aerodynamic package, which was a great opportunity given to me.

TABLE OF CONTENTS

LIST OF FIGURES

LIST OF TABLES

1. INTRODUCTION

This work is focused on the aerodynamic study of a Formula SAE race car, emphasizing on the underbody to get the maximum benefit of the ground effect, since the rest of the car is already designed and fixed. The car which is going to be the model studied throughout this thesis is the car for the season 2015 of TUW-Racing, which is the Formula SAE team belonging to Vienna University of Technology (TU WIEN).

In order to prove the existence of ground effect and its contribution to the overall downforce of any vehicle, two parallel studies of two-dimensional cases are developed. Specifically the flow around a symmetric and well known airfoil which has public data to contrast the own results to the official ones. Also the variation of the efficiency of the diffusor that will be given in function of its angle relative to the ground. The symmetric airfoil chosen is the NACA 0012 (400) and it is tested always with 0º angle of attack since the study of the airfoil efficiency variation is not the topic of this thesis.

First of all some general concepts about fluid dynamics focusing on aerodynamics, will be given to remember the required theoretical background and to understand everything related to the development of this work. Later it will be explained how car manufacturers improve the aerodynamic efficiency of their cars, by adding some aerodynamic devices using fluid dynamics principles.

Recent developments in computational fluid dynamics (CFD) and also computer technology have allowed the simulation of aerodynamics to accurately predict the downforce, flow patterns and many other features of the air flow around the vehicle. This simulation can greatly reduce the cost and time needed to test aerodynamic elements. In this work the design of a Formula SAE undertray is developed using CFD. So then a detailed view of the numerical calculations by CFD will be given, followed finally by results and discussions leading to the conclusions.

1.1. OBJECTIVE

The objective of this project is to design and develop aerodynamically the undertray of a formula style car. This implies a whole design of a new undertray that fits well to the overall design and performance of the rest of the car. This design includes the length, size and shape of the inlets and outlets of the diffuser as well as the shape of the conducts. To Increase the downforce and decrease the drag to be the fastest is the maximum absolute of any motor sport.

The objectives of this project are to:

- Test the ground effect influence on downforce.
- Design iterations of diffusers to get the most aerodynamically efficient.
- Optimize the diffuser geometry.
- Design a whole undertray for the car.
- CFD simulations of the whole car.

To make all of this possible knowledge about CFD is needed. Therefore 2D and 3D simulations of test cases and full car wind tunnel study will be developed.

1.2. TUW-RACING TEAM

TUW-Racing is the team of the Vienna University of Technology. It was founded in 2007 with competitive mind and EDGE MK1 was the first racing car of the team. TUW-Racing was the only team worldwide that successfully implemented a carbon fibre frame in EDGE 2 and also in EDGE3. Since EDGE 1 until EDGE 5 included, all the cars were motorized by a one cylinder KTM engine. From EDGE 6 the team powered the car by an electric motor. In 2015 the car was called EDGE 7 and it is the second self-developed electric car and mostly every component built in carbon fibre which makes it having a lightweight design.

1.3. FORMULA SAE COMPETITION

As it is already said the objective of the design and simulation in this thesis is for the participation on FSAE Competition. This competition challenges teams of different universities worldwide composed by undergraduates and graduate students to conceive, design, develop and test a small prototype formula style vehicle. Teams have a lot of design flexibility although they must always fulfil all the rules. The challenge is to develop a vehicle that can successfully compete in all the events described in the FSAE rules. Therefore it is a competition in which teams have the chance to demonstrate their engineering skills in comparison to the others around the world.

The vehicles should have high performance in terms of acceleration, braking and handling and be sufficiently durable to complete all the events described in the rules. Additional design factors to be considered are aesthetics, cost, ergonomics, maintainability, manufacturability and reliability. Each design is judged and evaluated against other competing designs to determine the best overall car. The cars are expected to be designed and fabricated under good engineering practices. Tests through which the cars are judged are clearly differentiated between static and dynamic events. Technical inspection, cost presentation, engineering design and high performance track endurance.

2. AUTOMOBILE AERODYNAMICS

2.1. HISTORY OF AERODYNAMIC DESIGN OF AUTOMOBILES

In the early days of automobile design there was nothing about aerodynamics. First cars had a box design (see figure 1) but they did not have to worry about aerodynamic efficiency because they were not so fast. One of the first ideas to shape the cars aerodynamically was the tear drop shape. The tear drop is the most aerodynamic shape that exists in nature although it is not true at all that a water droplet has that shape since it is spherical when falling down in free stream. Anyway the idea of the tear drop is clear and was implemented in some famous cars of that era. However one of the first cars that was designed with aerodynamic thought inspired by the geese V flight pattern was a complete commercial failure. Although it had balanced weight distribution on each axle and lower penetration into air resistance, its streamlined design was a big step ahead, the "Chrysler Airflow" (see figure 2) as it was called broke with the conventional car aesthetics of its time.

Figure 1. Ford T. (Source: www.caradisiac.com. Image by unknown)

Figure 2. Chrysler Airflow. (Source: www.google.com. Image by unknown)

As the race cars became even faster and due to the necessity of being the fastest on track, from racing came most of the improvements in automobile aerodynamics. From 1950s and 1960s engineers experimented with all kind of practices to design the best streamlined car. Cars were so fast already and the difficulty to handle them at high speeds increased. Then race cars aerodynamic design turned into a very precise science that engineers took very seriously as the results were in part depending on it.

Although the importance of it was already known, it was yet a very untested field, thus lot of improvements and devices came up quickly in order to increase downforce and try to decrease drag. Front and rear spoilers as in first instance and then some others like deflectors and special shapes to get the air flowing over the

top of the car. Companies started to develop their cars with aerodynamic shapes as streamlined as possible. But until 1980s came up these improvements were not applied to most vehicles for the common driver, only in racing. Audi changed this tendency and designed the Audi 100 with Cd of 0.30 (See figure 3). Nowadays it is nearly impossible to find a commercial car with any aerodynamic design on its bodywork (See figure 4). Unfortunately fabricating streamlined shapes is much complex as well as a Wind Tunnel is mandatory to have in order to test the vehicle.

Figure 3. Audi 100 (1983) had a drag coefficient of only 0.3. (Source: www.autoevolution.com. Image by Audi)

Figure 4. Audi A6 (2011-present) has a drag coefficient of only 0.26. (Source: motorburn.com. Image by Audi)

See reference [18] for more detailed information about automobile aerodynamics, from the earlier cars of 19th century until present on an illustrated review with many examples and also the catalogue [20].

2.2. AERODYNAMICS OF RACE CARS

Generating downforce is one development that has grown a lot in the last years. If you reduce the drag of the car you will go faster on straights, also if you can use the shape of the car to generate downforce then the car will also go faster around the corners. This means that a lightweight car will be able to make more efficient use of the tyres and will be able to accelerate faster in any direction. Although the top speeds are reduced due to the drag produced by aerodynamic devices, track lap times have improved.

A great inconvenience which caused some spectacular accidents during races was the fact that the streamlined shape at high speeds produced lift. So as the car became faster it became also more unstable in high speed corners. To avoid this automotive industry attempted to disturb the flow and spoilers. Spoilers do not eliminate drag but contribute to the downforce.

The revolution came with the implementation of the inverted wings to increase the tyre grip. Thanks to the inverted wings negative lift was produced (See figure 5).

Figure 5. Chaparral 2E 1966. Here one of the first attempts to build rear wings. (Source: www.tamsoldracecarsite.net. Image by unknown)

Figure 6. F1 Lotus Ford (1972) driven by Jochen Rindt. (Source: www.ausmotive.com. Image by unknown)

The cars literally lifted at some points depending on the speed and road conditions (See figure 6). Nowadays this is impossible because of the high downforce that the car generates.

Figure 7. Tyrrell P34 6 Wheeler driven by Jody Scheckter on 1976 season. (Source: en.espn.co.uk. Image by press association)

This 6 wheel design reduced the drag caused by the front wheels (See figure 7). Also increased the total contact path of the front tyres and created a greater swept area for the brake discs. Once the idea to keep the airflow over the top of the car was clear, Chaparral did another step forward: Ground effect.

Ground effect was introduced in early 1960's by Chaparral. Chaparral 1 was a car built that had an entire underbody shape like an inverted airfoil. Afterwards in 1969 a new race car with a revolutionary downforce concept that worked well was presented: the downforce produced

based on controlling the low pressure underneath the car. Chaparral invented a system with a big suction fan that independently of the speed of the car could control the pressure under the car (See figures 8 and 9). The periphery around the car and the ground was sealed. Also the air ejected by the suction fans helped to reduce the flow separation which improved the drag. As it might be expected, the design of this car was a success but such designs were outlawed immediately.

Figure 8. Chaparral 2J with ground effect. (Source: www.formula1-dictionary.net. Image by unknown)

Figure 9. Big suction fans to remove the air underneath the car used by Chaparral 2J. (Source: www.formula1-dictionary.net. Image by unknown)

Ground effects turned the car into large inverted wings and a very good example in Formula One was the Lotus John Player Special of the season 1978 (See figure 10). That car was exceptionally efficient and none knew why. Colin Chapman also known as the father of ground effect took this idea and made a car that was literally glued to the track without mechanical devices.

Figure 10. Mario Andretti in his Lotus (1978) with ground effect. (Source: www.formula1-dictionary.net. Image by unknown)

Inside the sidepods big inverted wings generated huge ground effect. This model also had sealed the sides between the ground and the sidepods in order to separate the low pressure area (See figure 11).

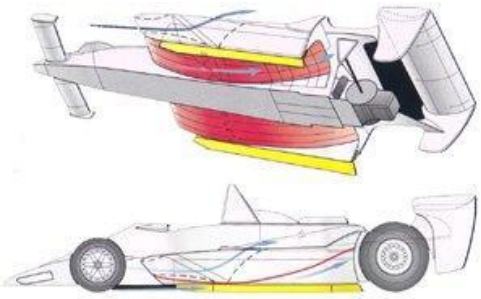

Figure 11. Illustration of the Inverted wings inside the sidepods. (Source: www.formula1-dictionary.net. Image by unknown)

2.3. AERODYNAMIC DEVICES ON RACE CARS

The design of aerodynamic elements for race car is complex due to the body interactions between these elements and the rest of the car. There are many aerodynamic elements implemented in cars. However the ones that contribute best to the downforce are inverted wings and underbody diffusers.

2.3.1. Front Wing

Front wing (See example in figure 12) is the most important element of the entire aero package. It is placed in front of the car and therefore is the first part of it that will be in contact with the air. The flow around the whole body shape car is mostly determined by this first contact existing at front wing. Front wing as well as the rest of the car is a generator of vortices. When a vortex separates from a solid surface it has a low pressure core. If the stream of these vortices is well oriented around the car they can be very useful in order to generate downforce and also acting as air curtains sealing other low pressure areas. If a front wing creates a turbulent wake or has a poor vortex generation then every component developed downstream of the front wing will have poor success.

Figure 12. Front wing of the F1 car Red Bull RB7 (2011). (Source: formula1techandart.files.wordpress.com. Image by unknown)

2.3.2. Rear Wing

The rear wing (See example in figure 13) is another crucial element for the performance of a Formula style race car. It is composed of more than one element and the low pressure area down the lower airfoil helps the diffuser to create more downforce. More wing angle increases the downforce and produces more drag and therefore reduces top speeds. That is the reason why Formula One teams use different rear wing configuration for each circuit. So in a track where high speed straights dominate less wing angle is set. Opposite to that larger angles of attack are set on tracks with many turns. The airfoil is normally split into separate elements. This is done for the reason that it reduces the flow separation caused by adverse pressure gradients. Also multiple wings produce more downforce than just one wing. The lift coefficient increases and lift/drag ratio decreases when increasing the number of aerofoils. The position of the wings relative to each other is important.

Figure 13. Rear wing of the Mercedes F1 car on 2012 season driven by Michael Schumacher. (Source: www.google.com. Image by unknown)

2.3.3. Gurney Flap

A gurney flap (See example in figure 14) is a simple piece of metal or carbon fibre rigidly fixed to the top of the trailing edge. The gurney flap is called like this because of Dan Gurney. This element basically operates by increasing pressure on the high pressure side of the wing, decreasing pressure on the suction side. This way helps the boundary layer stay attached all the way to the trailing edge on the suction side of the airfoil. Therefore flow separation is reduced.

Figure 14. Gurney flap at the trailing edge of a rear wing. (Source: www.google.com. Image by unknown)

2.3.4. Deflectors and Flip-Ups

Since a Formula style race car is an open wheeled car, wheels generate positive lift and this decrease the downforce produced by the whole car. Wheels also disturb the flow, so flip-ups (See figure 15) are designed to guide air over the wheels while at the same time create some downforce.

Figure 15. Detail of the body work of a Ferrari F1 where the flip-ups to guide the air over the back wheel can be seen. (Source: www.formula1-dictionary.net. Image by unknown)

Deflectors have no other function rather than guide the air (See figure 16). They are vertical surfaces following the bodywork shape. They can be used to guide the air into the radiators in order to help on the cooling and also to make the air follow the desired way.

Figure 16. Huge deflector at the side of this McLaren of 1994. (Source: www.google.com. Image by unknown)

2.3.5. Underbody

By shaping the underbody as an inverted wing, or with appropriate channels, or even with a simple scant angle that work with the Venturi effect, the overall pressure between the underbody and the ground decreases creating additional downforce.

2.3.6. Diffuser

The diffuser (See figure 17) in a race car is an area placed at the rear of the car. By the diffuser exits the air below the car.

Figure 17. Double diffuser designed for Brawn GP in 2009. (Source: everythingformula1.wordpress.com. Image by unknown)

3. INTRODUCTION TO AERODYNAMICS

Aerodynamics is the branch of fluid dynamics which is related to the study of air motion particularly when it interacts with a solid object. Therefore it is the study of the forces on a body which passes through air.

It is known that plane wings are designed for the purpose of elevating the plane from the ground. However, this thesis is not about planes but about a racing car, so on a racing car what is sought is the opposite effect that means sticking the maximum possible the car onto the ground thanks to the benefit of the aerodynamic vertical downward generated force known as downforce. The faster the solid body moves through air the higher the aerodynamic forces are, so then more downforce will aid the car keep rolling on the ground. Therefore a good aerodynamic design will allow the car go faster through the corners because of downforce and also faster on straights due to the reduced drag on movement direction.

Since the complexity of fluid mechanics is beyond of this thesis, this kind of introduction to fluid mechanics is only meant to be a quick summary of the most important concepts that will be stated along this thesis report. Main references of interest for further information are [1]-[7], [12], [14], [16], [17] and [19].

3.1. CLASSIFICATION OF FLOWS BY DIMENSIONLESS NUMBERS

A clear and standard way to classify any type of flow is through the dimensionless numbers. A dimensionless number is a number which has no physical dimension and give a clear idea of within which kind of physical case the fluid is described as well as to classify and compare the type of flow. Therefore, dimensionless numbers are widely used in fluid mechanics.

There are many dimensionless numbers meant to characterize flow such as Reynolds, Prandlt, Nusselt, Peclet, Mach, etc. Two of the more common and thus important dimensionless numbers to characterize any type of flow are Reynolds and Mach numbers.

3.1.1. Reynolds number

The most common dimensionless number used in fluid mechanics is the Reynolds Number (Re) which is defined as:

$$Re = \frac{\rho \cdot v \cdot L}{\mu}$$

Where,

ρ is density of the fluid (Kg/m^3)

v is the mean velocity of the object relative to the fluid (m/s)

L is the characteristic length (m)

μ is the dynamic viscosity of the fluid (Pa·s)

The characteristic length parameter is different for each flow type. For the flow within a pipe, the diameter of the pipe is used as a parameter. But for example for the flow around an airfoil the characteristic length will be taken as the length of the chord on a 2-dimensionsal case or the projected planform area on a 3-dimensions case. One of the main areas of interest for this thesis is the external flow around a car, and then the frontal projected area (normal to the direction of the velocity of the car) is used. Reynolds number represents the ratio of the inertial force to the viscous force. Therefore, a small Reynolds number implies that the viscosity is important and a large Reynolds number would mean that the inertial forces are more important. The critical Reynolds for a boundary layer flow at which the flow changes from laminar to turbulent is about Re=5·10^5.

3.1.2. Mach number

Another very common dimensionless number used in fluid mechanics is the Mach number (M) which is defined as the quotient between flow and sound speeds:

$$M = \frac{v}{c}$$

Where,

v is the velocity of the object relative to the fluid (m/s)

c is the speed of sound in the medium (m/s)

The Mach number allows describing the compressibility of a flow. Incompressible flow means that the flow is divergence free. This is the case when the density remains constant or its changes are imperceptible hence negligible. Air is considered incompressible when its velocity is lower than 0.3M, so incompressible flow limit is around 100m/s for a speed of sound of 340m/s. Compressible flow is then for flow speeds over 0.3M. The top speed of our car is obviously within incompressible flow range.

We can classify the flow by its Mach number:

- Subsonic flow: Speed of air is lower than the speed of sound, M<1
- Transonic flow: Speed of air is close to speed of sound, M=1
- Supersonic flow: Speed of air is higher than the speed of sound, M>1

Since we have already deduced that it an incompressible flow case (0.3M < 1M), then we can say that it is also a subsonic flow.

3.1.3. Aerodynamic coefficients (C_L and C_D)

Other two dimensionless numbers used in aerodynamics which are always must to state in any aerodynamic study are Lift and Drag coefficients (C_L and C_D).

C_L is the dimensionless coefficient used to quantify the lift of a body and it is defined as:

$$C_L = \frac{L}{q \cdot A}$$

Where,
L is the lift force,
q is dynamic pressure,
A is the reference area

C_D is the dimensionless coefficient used to quantify the drag or resistance of an object in a fluid environment and is defined as:

$$C_D = \frac{2F_d}{\rho \cdot v^2 \cdot A}$$

Where,
F_d is the drag force,
ρ is density of the fluid,

v is the velocity of the fluid relative to the body,
A is the reference area

From lift and drag coefficients can be calculated the aerodynamic efficiency. This is a term used to describe the relation between lift and drag.

$$Aerodynamic\ efficiency = \frac{C_L}{C_D}$$

It is easy to see that the lower the drag the better the aerodynamic efficiency.

3.2. AERODYNAMIC FORCE

Aerodynamic forces are generated around a solid body within a fluid with relative velocity to this fluid. The best way to give some ideas about aerodynamic forces is by using an airfoil as the solid body of study.

First of all, an airfoil is a wing shape seen in cross section. Streamlines are those imaginary lines that show the trajectory followed by the fluid around a solid body (See figure 18).

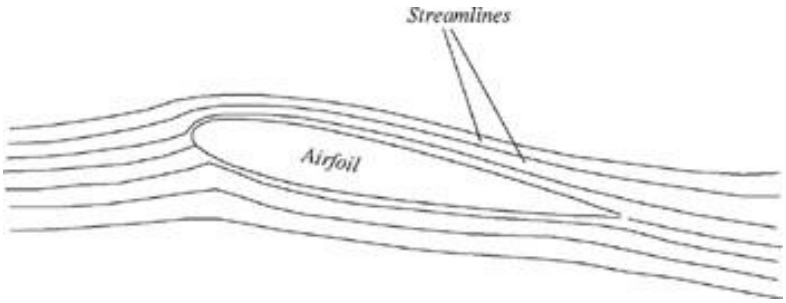

Figure 18. Streamlines around an airfoil. (Source: www.globalspec.com. Image by unknown)

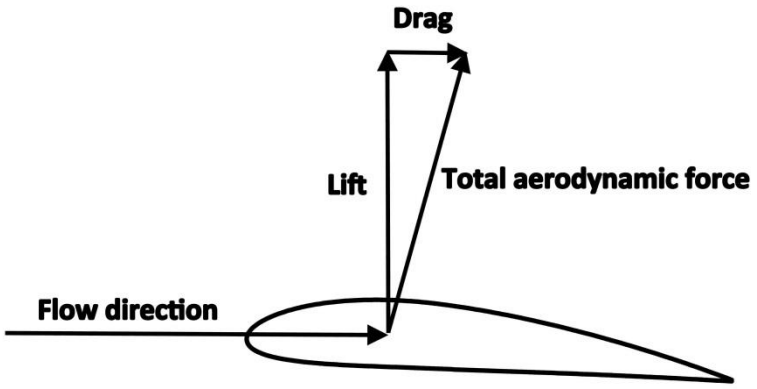

Figure 19. Aerodynamic forces around an airfoil. (Source: en.wikipedia.org. Image by unknown)

The relative wind to the airfoil splits and surrounds it all along the profile but due to geometry and according to fluid dynamics principles, the air has different velocity and pressure values depending on the side and the angle of attack. So around the airfoil we will find a low pressure area and a high pressure area. As the length of the upper side must be longer because of its curvature, the airflow will speed up in order to unite again with the airflow underneath the airfoil which is quite slower. Therefore, low pressure is on the upper side and high pressure area on the other side.

The gradient of a function is the direction of the steepest descent. Then the pressure gradient goes from the higher pressure to the lower pressure. In this case, by the airfoil position the vertical component of the aerodynamic total force goes in the upward direction and this aerodynamic force is known as Lift (See figure 19). There is also a horizontal force that is parallel to the airflow which is called drag and it means how much resistance to penetrate into air the airfoil has. Simplifying a little bit, this is the way how planes can lift and then fly. If lift is negative, then we have downforce. The shape of wing profile and its angle of attack influence the amount of lift.

These following scenes (See figures 20 and 21) have been calculated using CFD. And the results will be commented afterward in chapter 3.6.2.

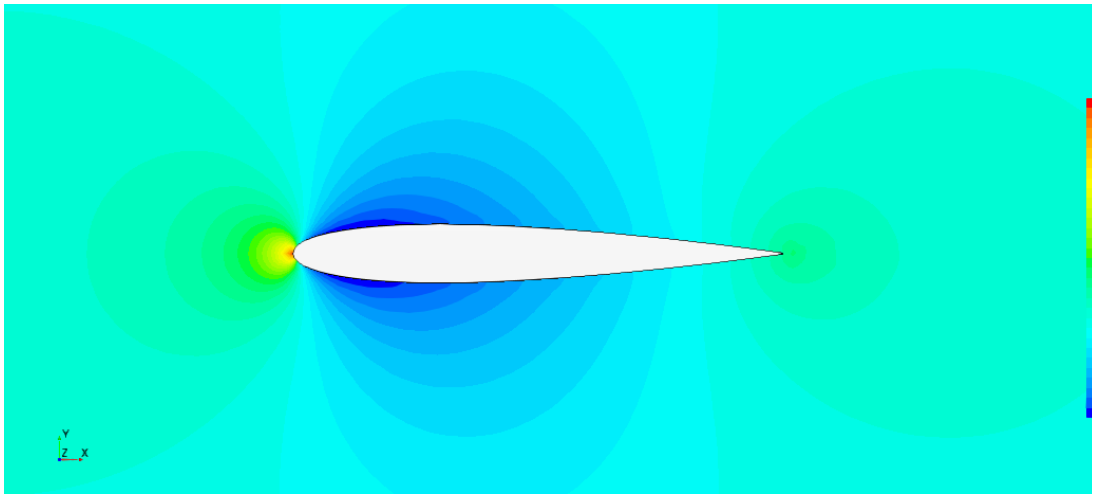

Figure 20. Scalar pressure field of the airfoil NACA 0012 in free stream.

In this case the airfoil has zero lift due to its symmetry.

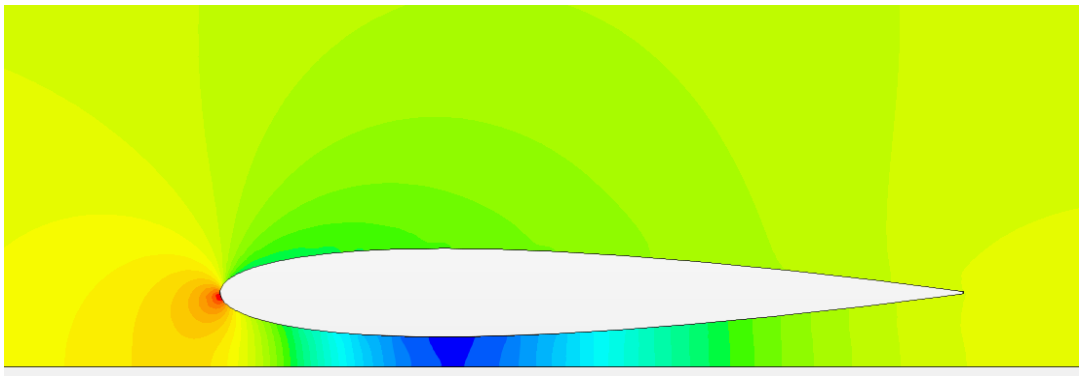

Figure 21. Scalar pressure field of the airfoil NACA 0012 near to the ground.

In this case the flow has to move faster underneath the airfoil to join with the upper flow at the trailing edge. This low pressure area generates a suction of the airfoil to the ground, thus it is subject to negative lift.

3.3. 2D-Potential Flow Theory

To describe the flow around the airfoil the study of the 2D-Potential flow theory is recommended.

By definition potential flow describes the velocity field as the gradient of the scalar function, which is known as velocity potential. A potential flow is characterized by an irrotational velocity field, which is a valid approximation for some applications.

For incompressible flow the velocity potential satisfies Laplace's equation and thus potential theory is applicable.

This and the following "Kutta condition" and "Kutta-Joukowski Theorem" are beyond the scope of the thesis and thus any further detailed information about potential flow theory can be found in literature [12], [14] and [16].

3.3.1. Kutta condition

The Kutta condition states that in a potential flow over a smooth and slender airfoil there is a stagnation point at the trailing. So the flow over the upper and lower surface of the airfoil for small angles of attack meets at the trailing edge smoothly (See figure 22). This condition imposes that the leading and trailing edges are stagnation points and the angle of attack must remain below the critical angle known as the stall angle. If the angle of attack exceeds the stall angle, then this condition is no longer applicable because the flow is not smooth and continuous anymore. Therefore the frontal stagnation point may change its position when changing the angle of attack. It is applicable to solid bodies which have sharp corners and steady flow. The Kutta condition is approximately satisfied in a high Reynolds number flow if the angle of attack is not too large. It is important in the practical calculation of lift on a wing

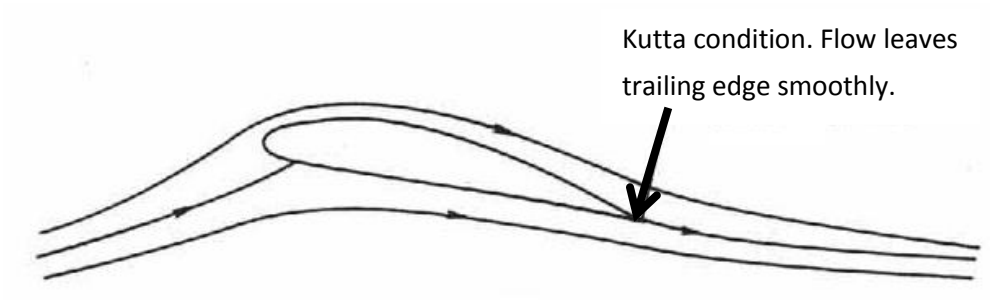

Figure 22. Inviscid flow over an airfoil with the Kutta condition applied. (Source: Figure 2 of the scientific paper [5])

3.3.2. Theorem of Kutta-Joukowski

This condition is significant when using the Kutta-Joukowski theorem to calculate lift generated by wing. The theorem refers to two-dimensional flow around an airfoil and determines the lift generated by 1 unit of span.

$$Lift = \rho \cdot \Gamma \cdot v$$

Where,

ρ is density

Γ is the circulation

v is the velocity of the free stream

The circulation Γ is defined as the line integral around a closed contour C enclosing the airfoil in the positive direction.

$$\Gamma = \oint_C V \cdot ds = \oint_C V \cdot cos\theta ds$$

For further detailed information see [14] and [5].

3.3. VISCOUS FLOWS

The viscosity of a fluid is a measure of its resistance to tangential deformations by shear stress. A fluid that has no resistance to shear stress is known as an ideal or inviscid fluid. So air flowing over a solid surface will stick to that surface. This phenomenon caused by viscosity is description of the no-slip condition. This so important condition for the correct set up of the simulation and the understanding of this problem, states that the velocity of the fluid at the solid surface equals the velocity of that surface. Regarding to the viscosity and shear stress, an important thing that will be analysed along the thesis that is crucial for the simulations is the boundary layer. Because of this viscosity phenomenon, a boundary layer whose velocity varies from zero at the wall surface to some relative value at some distance from the wall is formed. Regarding to the viscosity and shear stress, an important thing that will be analysed during this thesis that is crucial for the simulations is the boundary layer and the will to capture any behaviour of the air when it is really near to solid surface, most particularly for the undertray case on the ground surface.

Moreover, it is said that flow is on steady state when all external conditions to which it is subject to, such as velocity, pressure or density do not change over time. If those conditions change over time, it would be in transient state.

3.3.3. Navier-Stokes equations

The Navier-Stokes equations are the basic governing equations for a viscous fluid. These equations are obtained by applying Newton's second law to fluid motion. It is supplemented by the mass conservation equation (equation of continuity) and the energy equation. The Cartesian representation of the general form of the Navier-Stokes equations, with the velocity vector expanded as $u = (u_x, u_y, u_z)$ in the differential form is as follows:

X component direction:

$$\rho\left(\frac{\delta u_x}{\delta t} + u_x\frac{\delta u_x}{\delta x} + u_y\frac{\delta u_x}{\delta y} + u_z\frac{\delta u_x}{\delta z}\right) = -\frac{\delta p}{\delta x} + \mu\left(\frac{\delta^2 u_x}{\delta x^2} + \frac{\delta^2 u_x}{\delta y^2} + \frac{\delta^2 u_x}{\delta z^2}\right) - \mu\frac{\delta}{\delta x}\left(\frac{\delta u_x}{\delta x} + \frac{\delta u_y}{\delta y} + \frac{\delta u_z}{\delta z}\right) + \rho g_x$$

Y component direction:

$$\rho\left(\frac{\delta u_y}{\delta t} + u_x\frac{\delta u_y}{\delta x} + u_y\frac{\delta u_y}{\delta y} + u_z\frac{\delta u_y}{\delta z}\right) = -\frac{\delta p}{\delta y} + \mu\left(\frac{\delta^2 u_y}{\delta x^2} + \frac{\delta^2 u_y}{\delta y^2} + \frac{\delta^2 u_y}{\delta z^2}\right) - \mu\frac{\delta}{\delta y}\left(\frac{\delta u_x}{\delta x} + \frac{\delta u_y}{\delta y} + \frac{\delta u_z}{\delta z}\right) + \rho g_y$$

Z component direction:

$$\rho\left(\frac{\delta u_z}{\delta t} + u_x\frac{\delta u_z}{\delta x} + u_y\frac{\delta u_z}{\delta y} + u_z\frac{\delta u_z}{\delta z}\right) = -\frac{\delta p}{\delta z} + \mu\left(\frac{\delta^2 u_z}{\delta x^2} + \frac{\delta^2 u_z}{\delta y^2} + \frac{\delta^2 u_z}{\delta z^2}\right) - \mu\frac{\delta}{\delta z}\left(\frac{\delta u_x}{\delta x} + \frac{\delta u_y}{\delta y} + \frac{\delta u_z}{\delta z}\right) + \rho g_z$$

Where,

(u_x, u_y, u_z) are velocity components of the Cartesian reference system (x, y, z)

(g_x, g_y, g_z) are the gravity components of the Cartesian reference system (x, y, z)

$p\ is\ pressure$

$\rho\ is\ density$

The continuity equation looks like this:

$$\frac{\delta\rho}{\delta t}+\frac{\delta(\rho u_x)}{\delta x}+\frac{\delta(\rho u_y)}{\delta y}+\frac{\delta(\rho u_z)}{\delta z}=0$$

Where,

(u_x, u_y, u_z) are velocity components of the Cartesian reference system (x, y, z)

$p\ is\ pressure$

$\rho\ is\ density$

t is time

Incompressible flow

When the flow is incompressible, density does not change for any fluid particle and thus: $\frac{D\rho}{Dt}=0$.

Then the second part of the viscous terms of the Navier-Stokes equations fall away for incompressible flow

Therefore:

X component direction:

$$\rho\left(\frac{\delta u_x}{\delta t}+u_x\frac{\delta u_x}{\delta x}+u_y\frac{\delta u_x}{\delta y}+u_z\frac{\delta u_x}{\delta z}\right)=-\frac{\delta p}{\delta x}+\mu\left(\frac{\delta^2 u_x}{\delta x^2}+\frac{\delta^2 u_x}{\delta y^2}+\frac{\delta^2 u_x}{\delta z^2}\right)+\rho g_x$$

Y component direction:

$$\rho\left(\frac{\delta u_y}{\delta t}+u_x\frac{\delta u_y}{\delta x}+u_y\frac{\delta u_y}{\delta y}+u_z\frac{\delta u_y}{\delta z}\right)=-\frac{\delta p}{\delta y}+\mu\left(\frac{\delta^2 u_y}{\delta x^2}+\frac{\delta^2 u_y}{\delta y^2}+\frac{\delta^2 u_y}{\delta z^2}\right)+\rho g_y$$

Z component direction:

$$\rho\left(\frac{\delta u_z}{\delta t}+u_x\frac{\delta u_z}{\delta x}+u_y\frac{\delta u_z}{\delta y}+u_z\frac{\delta u_z}{\delta z}\right)=-\frac{\delta p}{\delta z}+\mu\left(\frac{\delta^2 u_z}{\delta x^2}+\frac{\delta^2 u_z}{\delta y^2}+\frac{\delta^2 u_z}{\delta z^2}\right)+\rho g_z$$

And the continuity equation:

$$\frac{\delta(\rho u_x)}{\delta x} + \frac{\delta(\rho u_y)}{\delta y} + \frac{\delta(\rho u_z)}{\delta z} = 0$$

Demonstrations and detailed explanations are widely given in classic literature, and for further information regarding to this see [12] and [14]. Also for further detailed information regarding to the Navier Stokes equations theory, numerical methods and descriptions of known results please see [19].

3.3.4. Turbulent flows

A turbulent flow is a flow regime characterized by chaotic property changes. Although not all chaotic flows are turbulent, turbulence is characterized by irregularity, high diffusivity which accelerates the homogenization of fluid mixtures. Vorticity in turbulent flows is not zero, and then turbulent flows are characterized by its rotationality and are also dissipative.

It is very important to study and be capable to characterize a turbulent flow since most of the flows in nature are in turbulent regime. Many engineering applications have to work also with turbulence (combustion chambers, heat exchangers, turbo machinery, chemical reactors, pipe flow, external flow around bluff bodies…) So it is a fact that most interest of flows in technology happen to be turbulent.

See reference [17] for detailed information and also other more general publications such as [12] and [14].

3.3.5. Boundary-Layer concept

The boundary layer is the layer of fluid right next to the surface where the effects of viscosity are significant. The viscosity of the airflow reduces the local velocities on a surface (See figure 24) and is responsible for skin friction. Using the boundary layer concept at high Reynolds number flows then can be decomposed into an inviscid potential flow and a boundary layer flow.

There are two types of boundary layer flow: laminar and turbulent.

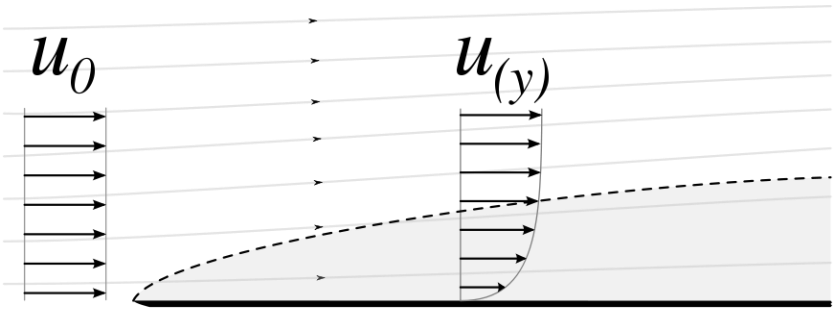

Figure 23. Boundary layer. (Source: Wikipedia. Image by unknown)

The laminar boundary layer is a very smooth flow while the turbulent boundary layer contains swirls. Boundary layer flow over a wing surface begins as laminar flow but at some distance from the leading edge, the smooth laminar flow breaks down and changes to a turbulent flow. See further information in [2].

3.4. GROUND EFFECT

In racing cars, ground effect is a term applied to a series of aerodynamic effects used in car design, which has been exploited to create downforce. It can be explained through Venturi effect.

3.4.1. Venturi Effect

This effect is also explained through other two principles, Bernoulli's principle and Continuity equation:

Equation of Bernoulli

Bernoulli's principle states that for an inviscid flow, an increase in the speed of the fluid occurs simultaneously with a decrease in pressure or a decrease in the fluid's potential energy. There are different forms of the Bernoulli equation for different types of flow, but in this case the simple form of the Bernoulli equation is valid because we are working with an incompressible flow.

Simple form of Bernoulli's equation:

$$\frac{V^2}{2g} + \frac{P}{\rho g} + z = constant$$

Where:

v is velocity (m/s)

p is pressure (Pa)

g is acceleration of gravity (9.8m/s2)

ρ is density (kg/m3)

z is height (m)

Equation of continuity

This equation states the behaviour of a flow within a conduit. If inside this conduit there are no entrances or sinks, we can assume that the incoming mass flow in the conduit is equal to the outgoing. From the mass flow formula, we can see that for an incompressible fluid, such as air at lower speeds to 0.3M, if the duct area increases the speed flow decreases and vice versa. For incompressible flows:

$$\frac{\Delta m_{in}}{t} = \frac{\Delta m_{out}}{t} = \frac{\Delta m}{t} = \rho A v$$

$$\rho_{in} A_{in} v_{in} = \rho_{out} A_{out} v_{out}$$

$$A \cdot v = constant$$

So we can deduce that area and velocity are inversely proportional.

Where m is mass (Kg), t is time (s), ρ is density (Kg/m3) which we assume constant because of the incompressible flow approximation, A is area (m2) and v is velocity (m/s).

Once Bernoulli and Continuity equations are explained and understood venturi effect can be introduced:

Basically it states that for a flow within a conduct its velocity increases and its pressure decreases when it passes through a smaller section. This is also the reason of the ground effect generation, the main objective of this project by designing an efficient underbody and diffuser. Giovanni Venturi discovered this effect thanks to an experiment he made with a tube (See figure 25) that nowadays has his name. If we take a look at the tube of Venturi, we will see how it exactly works and why the car is suctioned onto the track by ground effect:

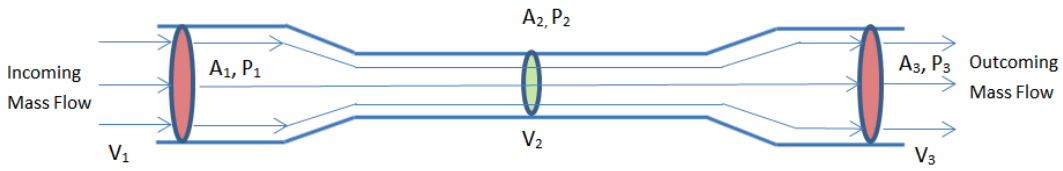

Figure 24. Venturi tube.

As it is showed in the picture above, the duct has a convergent-divergent shape with a smaller section in the middle (A_2). The fluid pressure is notably reduced by the middle section due to the increase of velocity which implies the decrease of the pressure according to the principles announced before ($A \cdot v$ = constant). So in fluid dynamics, a fluid's velocity must increase as it passes through a constriction according to the principle of continuity because mass flow has to be the same at the inlet so as it is at the outlet. Thus any increase of kinetic energy (which occurs in the middle section) is balanced by a drop in static pressure.

Then we can have suction from the high pressure gradient and these are the very basics of what we seek in order to stick the car onto the ground.

Once equations of Bernoulli and Continuity are understood, we can go one step further and focus on the real aim of this thesis. We are going to emphasize the ground effect and the device that mostly generates it: the undertray and its rear diffuser.

The finality of an undertray is to generate ground effect thanks to the close proximity of it to the ground. It can be said that ground effect is a kind of Venturi effect under the vehicle. As in a venturi tube, the cross section of the underneath the car region has three differentiated areas which make the difference between a good aerodynamic underbody design and a poor one. In the front part of the car, there is like an inlet nozzle which increases the velocity of the air underneath the car. After this nozzle there is a constrain area where the maximum velocity is reached and finally on the back we have the diffuser, where the air is slowed down again to the

free stream velocity. By Bernoulli's Equation, as the local velocity increases the local pressure decreases. Thus, there is a low pressure area underneath the car where the air is speed up and a higher pressure on the top. This pressure difference creates a resultant force whose direction is from the high pressure to the low pressure, so downforce is generated. It is known that the efficiency of the venturi tube is as good as the efficiency of the diffuser section is. For this reason we can state that the efficiency of an undertray is as good as its diffuser section is. Although it is a venturi like effect, since it is an open system it is false to state that the diffuser of the undertray expands the air as it would mean that the density is changing. However it is true that the diffuser angle determines the efficiency of the undertray performance.

A low pressure peak is located at the entrance of the diffuser. To know the location of this low pressure peak it is important in order to balance the centre of pressure of the undertray. By changing its location rearward or forward the centre of pressure is moved. Obviously, a race car must be balanced because if it is not then the performance can be seriously affected at high speeds.

Back to the angle of the diffuser relative to the ground, the best theoretical performance would be with the highest angle possible without flow separation because the bigger the chamber of the diffuser to slow down the air is, the lower the pressure underneath the car can be. However if separation occurs then the downforce is reduced and drag increased. Due to this, different 2-dimensional simulations of the cross sectional areas of the undertrays have been done. In 2-dimensional simulations it is showed that the maximum downforce reached is with an angle of 6º. Anyhow, in 3-dimensional behaviour it changes a little bit due to the influence of the vortices formed at the entrance of the undertray and they go all along low pressure area decreasing the pressure. Technically it should allow to design diffusers with larger angles.

After knowing all these concepts, the undertray is designed in order to get the maximum efficiency. An important thing to deal with is that the car and the rest of the aeropackage is already designed and fixed for this season, so the undertray must get the maximum downforce dealing with the current design.

3.4.2. Ground effect of a 2D airfoil

To calculate the lift around an airfoil by a different method than CFD exist the panel methods. Panel methods are techniques for solving incompressible potential flow over thick 2D and 3D geometries. For the 2D case of an airfoil, its surface is divided into piecewise straight line segments or panels and vortex are placed on each panel. To apply panel methods some assumptions have to be taken such as inviscid, incompressible, irrotational and steady.

Further information can be found in [12], [14], [4] and [16].

Method of images

For the specific case of the airfoil near to the ground method of images is applied. This method is a mathematical tool for solving differential equations in which the domain of the sought function is extended by the addition of its mirror image with respect to a symmetry plane (See figure 26).

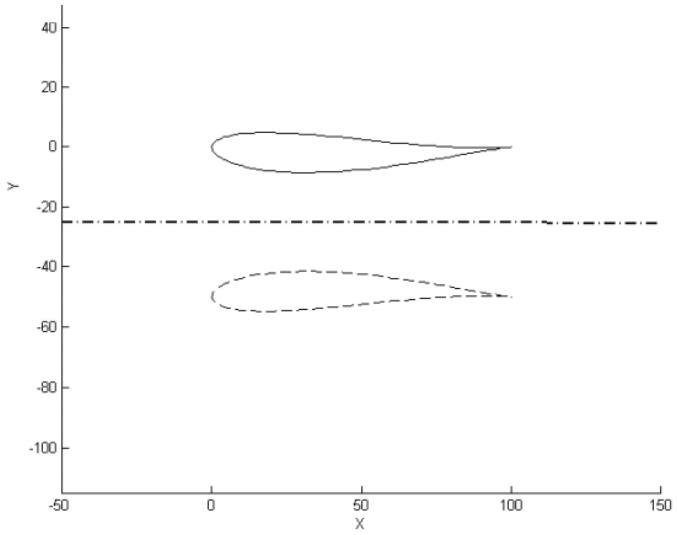

Figure 25. Method of images representation for an airfoil. Y direction represents the parameter c/h. Y direction represents the parameter c/h. (Source: Figure 3 of the reference [16]. Image by Diogo Matos Chaves)

For further information see Low speed aerodynamics and Paper Implementation of 2D Panel Method for Potential Flow Past Multi-Element Airfoil Configurations

2D Airfoil CFD simulations and results

To verify that the meshing and choice of turbulent model are reasonable and that we can trust the numerical solutions for the main problem, the numerical study of the 2D flow around a known airfoil such as NACA 0012 (400) near to the ground compared to current existing scientific data [4] will be developed. This study will test the influence of the ground effect on the aerodynamic characteristics of this airfoil on 0º angle of attack, such as lift and force coefficients (CD and CL) as function of the Reynolds number.

It is a parametric study of the airfoil NACA 12 (400) with 0º angle of attack in free stream and under the influence of ground effect. For the parametrisation of the influence of the ground effect on an airfoil the ratio between the height h from the leading edge to the ground and the length of the chord c has been used. In order to see the dependence of the force coefficients on the Reynolds number ($Re = v \cdot \frac{c}{\mu}$) and on the ration h/c the free stream velocity and the ground distance have been varied. All the simulations related to the ground effect have been set up with moving no-slip ground at the same velocity of the air and a low y+ wall treatment. For the simulations in free stream the airfoil has been set into the middle of the domain far from any wall and low y+ wall treatment as well (See figure 27).

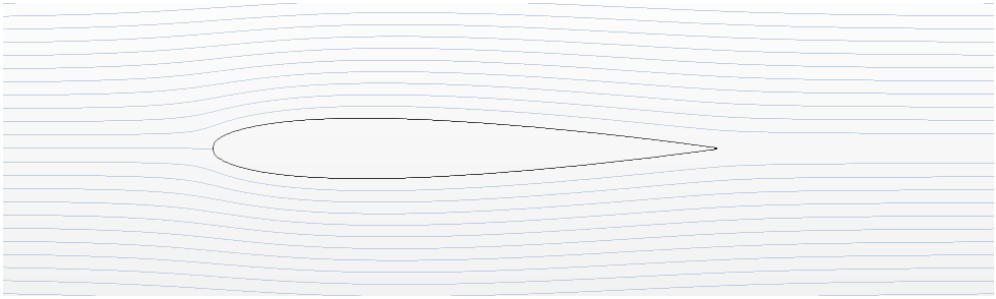

Figure 26. Streamlines of the airfoil NACA 0012 in free stream.

Airfoil on ground effect:

It is stated that aerodynamic efficiency increases with ground proximity, therefore the results in this section confirms this statement. This numerical study has been compared to the results of the study [4].

As it is NACA 0012 (400) the chord is 0.4m long so is the planform area. Velocity of the free stream is v = 20m/s, Re = $5.1 \cdot 10^5$. Also air density used for the calculations is ρ = 1.18415 kg/m^3 and dynamic viscosity μ = $1.85508 \cdot 10^{-5}$ Pa·s.

See table 1 for boundary conditions of the computational domain:

Boundary	Condition
Inlet	Velocity Inlet(free stream Velocity)
Outlet	Pressure Outlet (0Pa)
Top	Symmetry plane (far away from the upper side of the airfoil)
Ground	No Slip Condition – Moving ground. Same speed of the free stream

Table 1. Boundary conditions for the 2D airfoil on ground effect.

Below is presented the acquired data as a function of h/c:

h/c	CL	CD	CL/CD
0,1	-0,574	0,029	20,123
0,2	-0,253	0,018	14,323
0,3	-0,118	0,016	7,471
0,4	-0,063	0,015	4,173
0,5	-0,036	0,015	2,440
0,6	-0,023	0,014	1,591
0,7	-0,014	0,014	0,997
0,8	-0,012	0,014	0,847
0,9	-0,007	0,014	0,467
1	-0,007	0,014	0,477
1,1	-0,004	0,014	0,307
1,6	-0,003	0,014	0,179
2	-0,002	0,014	0,167

Table 2. CL and CD of the airfoil NACA 0012 as a function of h/c. Re = 5.1•105.

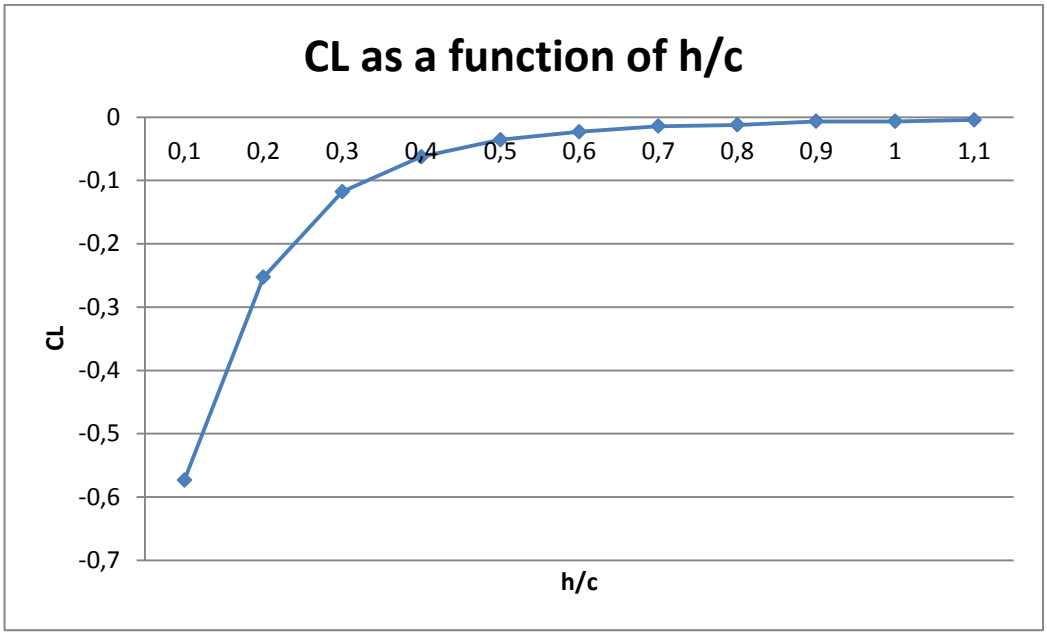

Figure 27. CL vs h/c.

It is shown that as the airfoil gets closer to the ground its downward pressure is notably increased. Drag coefficient is parametrized with Reynolds (See table 3).

Reynolds	CL	CD	CL/CD
2,55E+04	-0,19	0,04	5,01
9,70E+04	-0,20	0,03	7,42
1,28E+05	-0,21	0,02	8,35
2,55E+05	-0,22	0,02	10,71
3,83E+05	-0,24	0,02	12,55
5,11E+05	-0,25	0,02	14,32
7,66E+05	-0,26	0,02	15,87
9,70E+05	-0,27	0,02	17,27
1,02E+06	-0,27	0,02	17,66
1,28E+06	-0,27	0,01	18,39
1,53E+06	-0,28	0,01	19,31
1,79E+06	-0,28	0,01	19,92
2,04E+06	-0,28	0,01	20,91
2,30E+06	-0,28	0,01	21,19
2,55E+06	-0,29	0,01	22,34
5,11E+06	-0,30	0,01	25,80
9,70E+06	-0,30	0,01	29,44

Table 3. CL and CD of the airfoil NACA 0012 as a function of the Reynolds number.

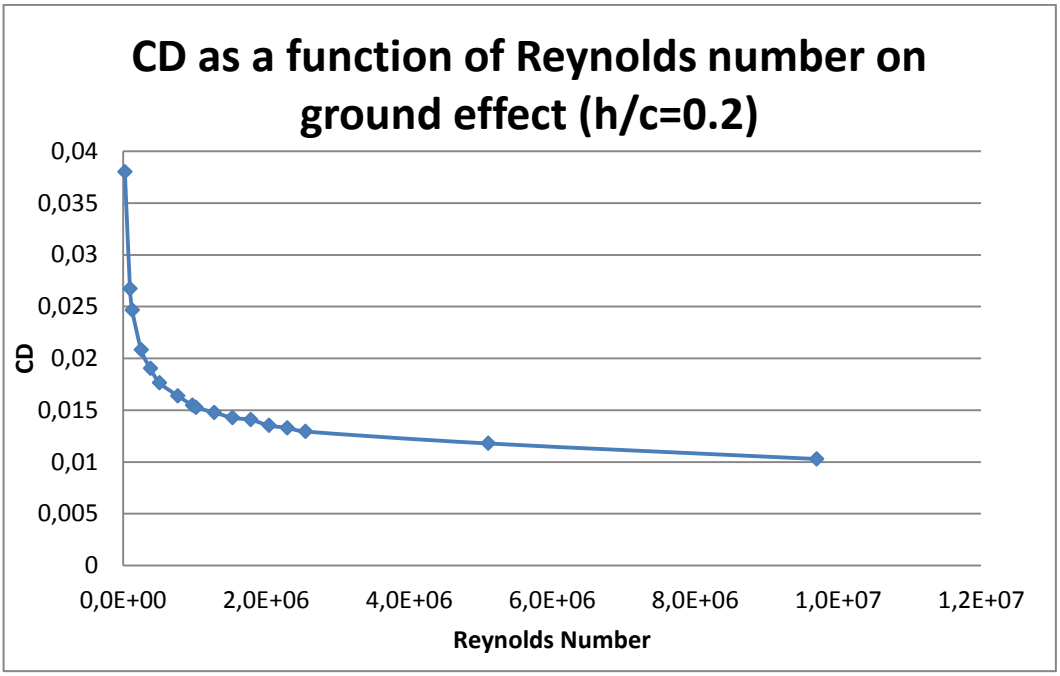

Figure 28. CD of the airfoil NACA 0012 in ground effect (h/c=0.2) as a function of Reynolds number.

It can be appreciated that in case of turbulent flow, CD decreases logarithmically as the Reynolds is increased. It is due to the boundary layer theory and it can be explained by the boundary layer on a flat plate case [2].

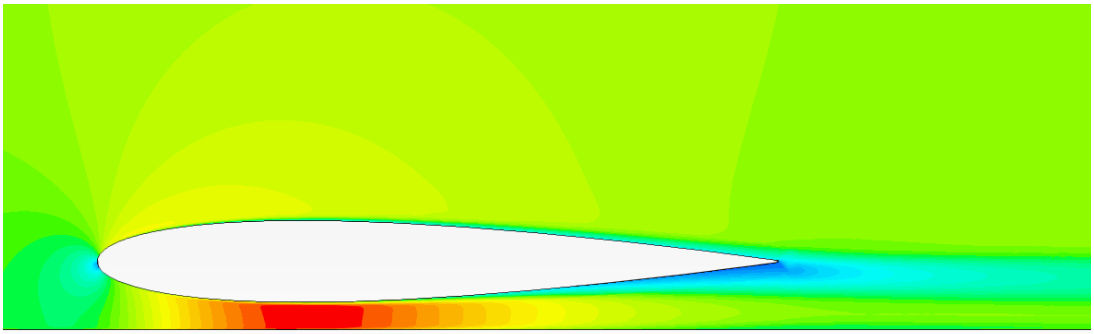

Figure 29. Velocity field of the NACA 0012 near to the ground.

Airfoil in free stream

The same test is done for the case of the airfoil in free stream. Boundary conditions are given in table 4 and results in table 5.

Boundary	Condition
Inlet	Velocity Inlet(free stream Velocity)

Outlet	Pressure Outlet (0Pa)
Top	Symmetry plane (far away from the upper side of the airfoil)
Ground	Symmetry plane (far away from the down side of the airfoil)

Table 4. Boundary conditions for the airfoil in free stream.

Reynolds	CL	CD	CL/CD
9,70E+04	-3,40E-04	0,023	-0,015
1,28E+05	-1,94E-04	0,021	-0,009
2,55E+05	-2,40E-04	0,018	-0,013
5,11E+05	-5,50E-04	0,015	-0,037
7,66E+05	-7,70E-04	0,014	-0,055
1,02E+06	-9,47E-04	0,013	-0,070
1,28E+06	-1,05E-03	0,013	-0,081
1,53E+06	-1,00E-03	0,012	-0,083
2,04E+06	-1,39E-03	0,012	-0,115

Table 5. CL and CD vs Reynolds. For airfoil NACA 0012.

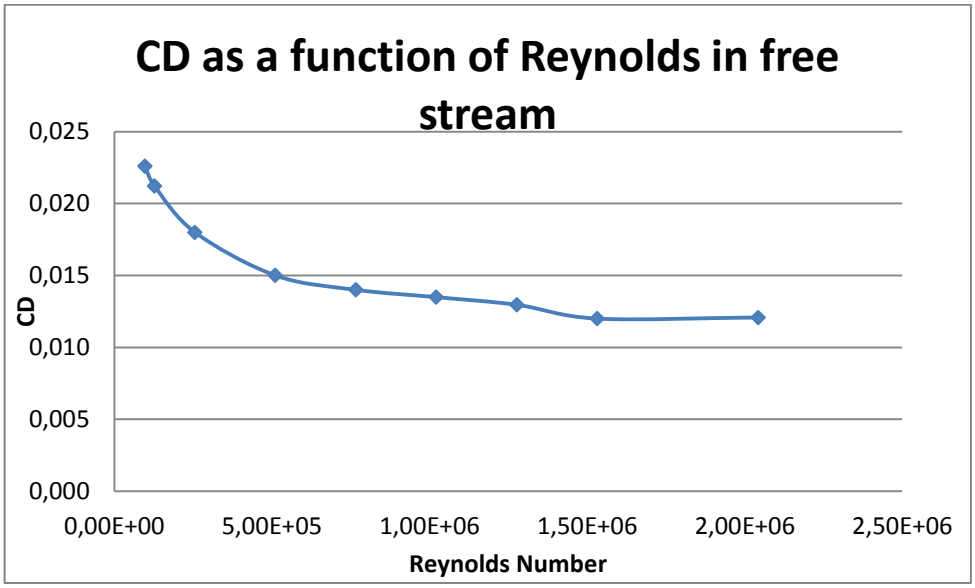

Figure 30. CD as a function of Reynolds in free stream for the airfoil NACA 0012.

It is stated that CL has no lift and this little amount of lift calculated is because of a small numerical error.

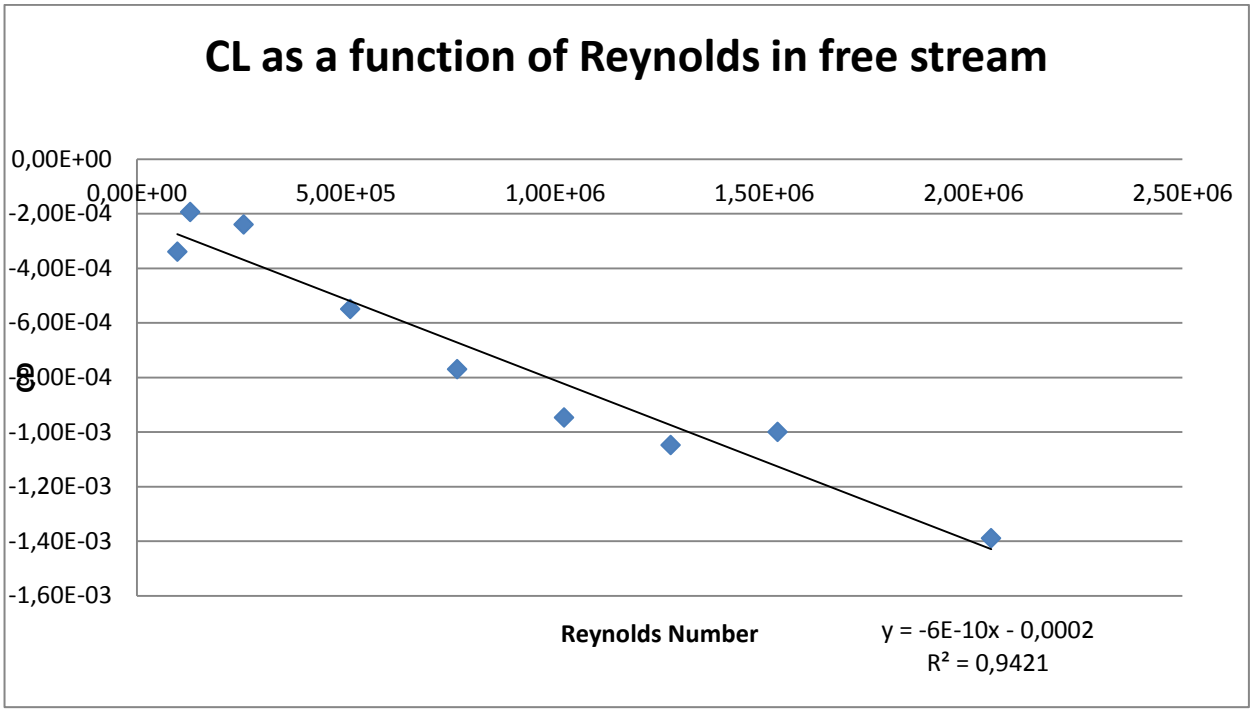

Figure 31. CL vs Reynolds number in free stream for the airfoil NACA 0012.

Since NACA 0012 is a symmetric airfoil and in this case is studied in free stream, it should have zero lift. From the plot above, we can see that the CL is almost 0.

4. AERODYNAMIC SIMULATIONS OF RACE CARS USING CFD

CFD technology can simulate the flow around the vehicle and the obtained solution allows us to observe different fluid properties such as pressure, velocity, aerodynamic forces around the car (lift and drag) and many others.

On CFD model, usually we work with geometry imported from CAD software. Depending on what is of interest and the required accuracy for the results as well as the computing power available, the imported model can be more or less complex. The wind tunnel to generate the flow is a box placed around the car and its size defined in function of the size of the geometry. The full 3D CAD model of the car is designed with CATIA V5 as it is the software used in the TUW Racing Team.

The software used in the Aerodynamics department of TUW Racing Team for the 2015 season is Star CCM+ 9.06.011. This software provides a powerful all-in-one solution which means that one only software is needed for pre-processing, calculation and post-processing.

Since the main aim of this thesis is the undertray, and its function is to generate downforce thanks to the clearance to the ground, another important thing to verify is the efficiency of the diffuser geometry. Once in the diffuser, the accelerated flow coming from the constrained region underneath the car will be decelerated. Therefore, different angles of diffuser will need to be studied to find the most efficient.

In this chapter will be detailed the settings of the simulations and chosen models after the studying of the 2D flow around NACA 0012 profile.

4.1. COMPUTATIONAL FLUID DOMAIN

First of all, the 3D CAD model has to be imported into Star CCM+ and the geometry needs to be cleaned up because it may have many surface errors such as not closed volume, overlayed surfaces, intersecting surfaces and so on. If the surface geometry is not cleaned up the surface mesher won't be able to work with it. Once all the car surfaces are clean then the fluid domain can be created. It basically consists on the car within the wind tunnel and the dimensions of this domain are very important so have to be set according to the standards found in the literature. To define the fluid domain in dimensions and to set proper boundary conditions is something that should be taken seriously.

In the user guide of Star CCM+ there are some useful articles relevant to the settings of the fluid domain for external flow around a ground vehicle which show the most efficient and good practices to get a reliable simulation [10]],[11].

Size of the domain around the car

Before starting to define boundary conditions, first it is needed to have the working fluid domain geometrically configured. For an external flow simulation study, the fluid domain is obviously a Wind Tunnel which is basically a horizontal prism resting on the ground and tangent to the vehicle wheels in this case. It can be split by faces in order to set each boundary condition on them as follows: inlet, outlet, ground, top, wall and symmetry plane.

To estimate how much domain you need is used the blockage ratio. The blockage ratio is the ratio between frontal area of your car and cross section of the full domain. This ratio should be always less than 0.2% as found in literature for open road condition.

$$Blockage\ ratio = \frac{Car\ frontal\ area}{Domain\ cross\ section\ area} < 0.2\%$$

Anyhow, the recommended minimum domain size for On-Road Simulations is how this picture below shows (See figure 33):

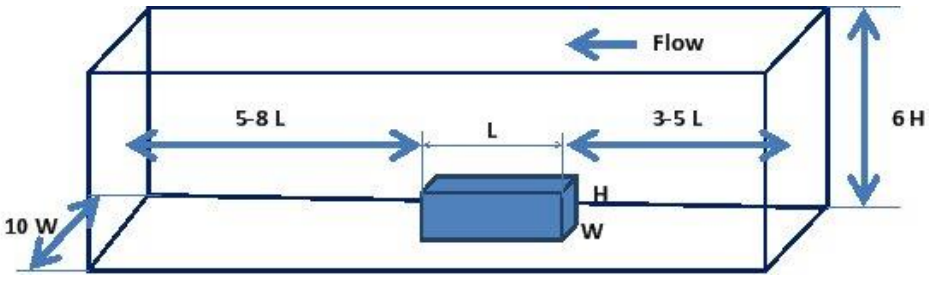

Figure 32. Typical outer domain sizes for a wind tunnel simulation. (Source: Star CCM+ User Guide. Image by CD-ADAPCO).

1.

Car dimensions

From figures 34 and 35 car dimensions are obtained:

Height: 1.28m Width: 1.42m Length: 3m

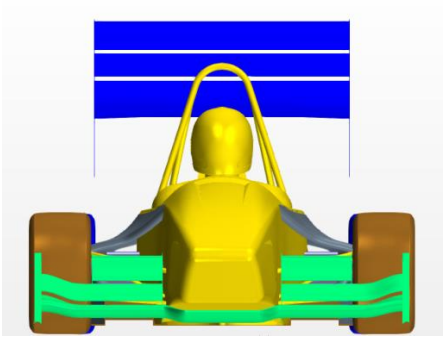

Figure 33. Frontal view of the car.

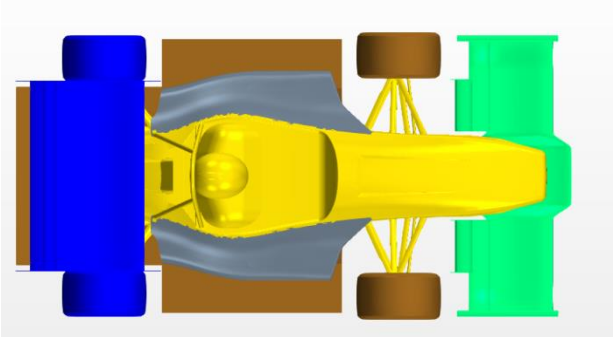

Figure 34. Planform view of the car.

According to this, the domain size and therefore the wind tunnel size is as follows:

Dimension	Value
Height	7m
Width	7m
Length	28m
Frontal Area	0.503m^2
Domain cross section area	196m^2

Table 6. Dimensions of the computational domain.

Note that in order to minimize the cell count and so the time needed for calculations, the model is cut by a symmetry plane (See the computational domain in figure 36).

Wind tunnel blockage ratio

Therefore, the blockage ratio of the wind tunnel is:

$$Blockage\ ratio = \frac{0.503}{196} = 0.26\%$$

Although that this Blockage ratio is a little bit higher than 0.2%, it is taken as good enough due to the limited computing resources.

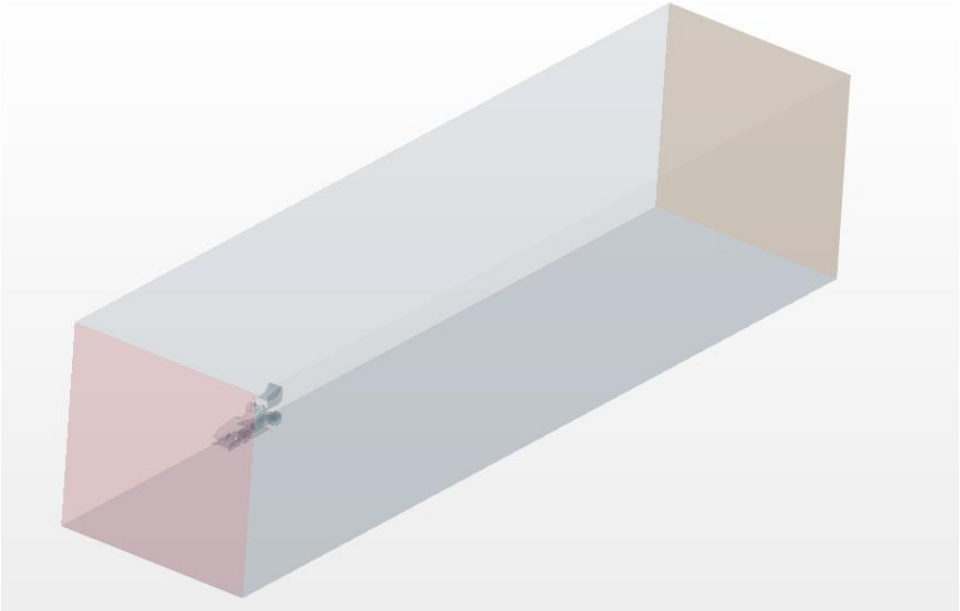

Figure 35. General view of the simulation domain.

4.2. BOUNDARY CONDITIONS

One of the most important things to do with precision besides to get a really fine and accurate mesh generation and choosing the proper physical models to run the solution is to define the boundary conditions of the domain.

At this point, it is very important to know and understand all the possibilities that exist to define the boundary conditions of the problem, which will affect considerably to the solutions depending on how close it is to the reality. Therefore this section is about how these conditions are defined for this external flow study and why these are the chosen ones. It is also very important to think about the computer resources available for this thesis, so boundary conditions shall be wisely configured to get the best balance between accuracy of the solution and the required calculation time to reach the closest approximations of what is actually happening in an on road car operation.

Since the simulation is of an open wheeled car on moving ground the tyres must be rotating. The simulation of the tyres is necessary because they are critical points of positive lift and generate a lot of turbulence that affect to the air around the rest of the car.

4.2.1. Shear conditions at walls

Shear stress

A shear stress, denoted τ is defined as the component of stress coplanar with a material cross section. Shear stress arises from the force vector component parallel to the cross section. Normal stress, on the other hand, arises from the force vector component perpendicular to the material cross section on which it acts.

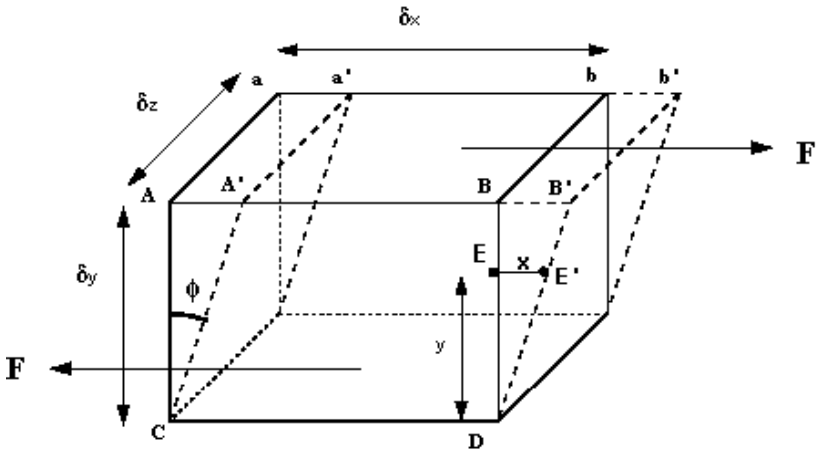

Figure 36. Representation of shear stress on the elemental cube.

As shown in the picture above (See figure 37), a shearing force is applied to the top of the elemental cube while the bottom is held in place. The resulting shear stress τ deforms the cube.

Shear stress in fluids

Any fluid moving along solid boundary will cause a shear stress on that boundary.

For all Newtonian fluids in laminar flow the shear stress is proportional to the strain rate in the fluid where the viscosity is the constant of proportionality. The shear stress is imparted onto the boundary as a result of this loss of velocity. The shear stress, for a Newtonian fluid, at a surface element parallel to a flat plate, at the point y, is given by:

$$\tau(y) = \mu \frac{\delta u}{\delta y}$$

Where,

μ is the dynamic viscosity of the fluid;

u is the velocity of the fluid along the boundary;

y is the height above the boundary.

Wall Shear Stress

It is of great interest for the simulation, knowing the shear stress incurring on the walls, which is known as Wall shear stress and it is a specific case when the distance from the fluid to the wall is zero.

Specifically, the wall shear stress is defined as:

$$\tau_w = \tau(y = 0) = \mu \frac{\delta u}{\delta y} \; for \; y = 0$$

Since the software used, Star CCM+ brings two "shear stress condition" options, these are the ones subject to be analysed in order to choose the best approximation for this case.

- **Slip:** No shear stress at the wall.
- **No-Slip:** Adds tangential velocity specification

The slip wall condition indicates that there is no shear stress at the wall and that the relative velocity of the air to the boundary wall is not zero.

The No-Slip boundary condition states that a moving fluid in contact with a solid body will not have any velocity relative to the body at the contact surface. This condition of not slipping over a solid surface has to be satisfied by a moving fluid. The idea is that the normal component of velocity at the solid wall should be zero to satisfy the no penetration condition. In the case of fluids the tangential velocity is also zero at the wall.

So the slip wall condition is for cases where viscous effects at the wall are negligible and/or your mesh size is much bigger than the boundary layer thickness (so you are not capturing the boundary layer effects anyway). The slip boundary is also the proper boundary condition for symmetry surfaces.

Then for an open road simulation, the ground should be specified as moving at the vehicle speed, whereby the side and top walls modelled with slip wall boundary conditions. The speed of the vehicle is then applied to the inlet with a pressure outlet used at the exit of the wind tunnel.

4.3. MESH GENERATION

A mesh is the discretized representation in cells of the computational domain. A cell is an ordered collection of faces that defines a closed volume in space.

It is widely known that the mesh is probably the most important phase in the CFD workflow process. For this reason most of the time spent on this thesis has been taken by the mesh generation. In this section some facts about types of mesh and everything related to the mesh will be given. The most proper types of mesh and configuration as well as good practices developed to get a fine mesh for external flow around a car will be commented upon.

To have a good quality mesh will determine the accuracy and stability of the numerical computation. The base mesh size chosen around the car was 24mm and the minimum cell size allowed 3mm with a smooth growth which was enough to capture all the flow details around the vehicle. Volumetric refinements were created in order to capture well the wake generated behind the car and ground effect on the underbody, surface refinements for every part of the car (monocoque, sidepods, suspensions, wheels, frontwing, rearwing and undertray). This is done to avoid losing detail on the surface and so near the walls. Mesh grows as it goes away from the car and refinements reducing the cell count where the detail is not important. The prism layer mesh consist of 8 layers all over the domain with a first near the wall layer thickness of only 0.1mm, which allows to have a low Wall Y+ all around the car surface that in average almost the whole surface under the value of 5. So we have a very fine wall treatment to capture near the wall effects such as viscous layer shear stress (See figures 38 and 39 for mesh detail views).

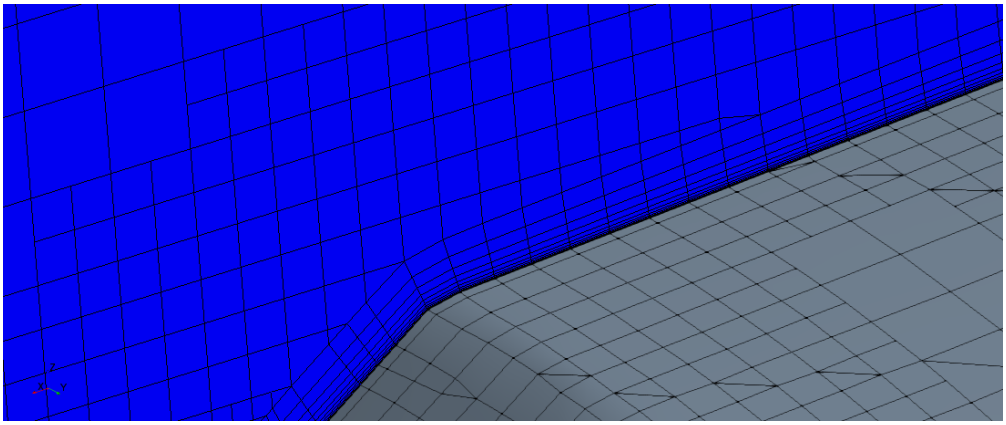

Figure 37. Prism layer mesh detail.

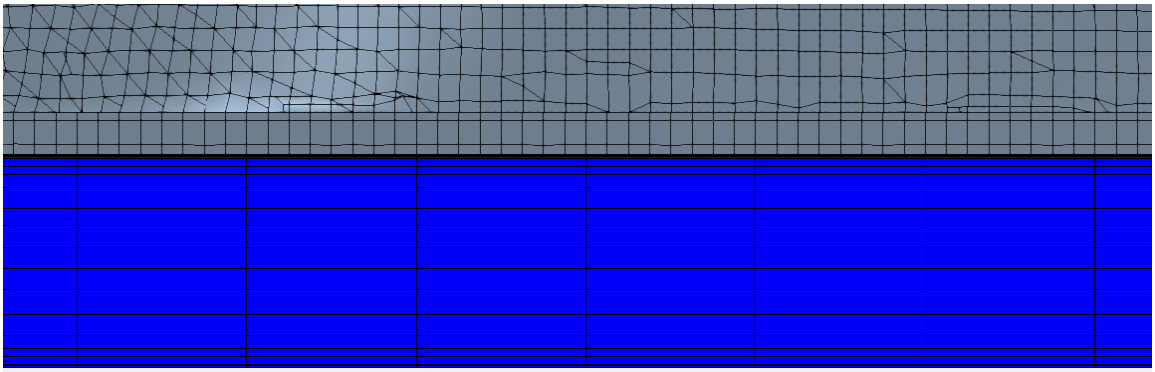

Figure 38. Below the car refinement detail.

The boundary layer around the car has to be resolved properly and it requires high grid resolution where near the surface. Cell density is variable and depends on many factors. But in fact, comparing turbulent to laminar flows it is very clear that for turbulent flows the numerical results are more dependent on grid density, due to the strong interaction of mean flow and turbulence.

4.3.1. Mesh Types

Surface mesh

Surface mesh is the one that will remesh the 3D CAD model from its poor quality to the new fine remeshed surface and it has direct influence on the quality of the resulting volume mesh. Therefore the generation of this mesh should be considered carefully (See figure 40).

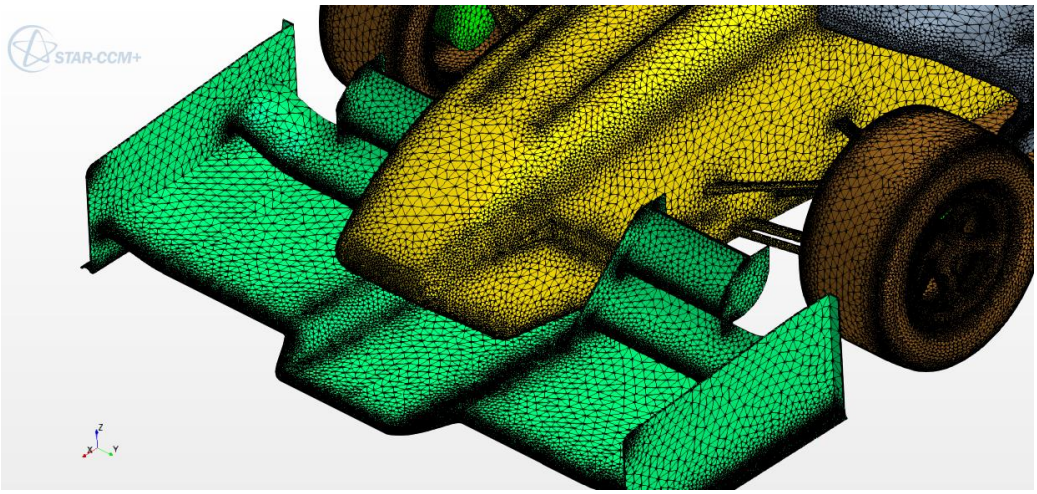

Figure 39. Surface mesh detail of the front side of the car.

Volume Mesh

The volume mesh is the discretized by cells representation within the space of the volume of an object. It can be discretized in different ways. Star CCM+ provides five types of volume meshes. However, the most used and typical for external aerodynamics are polyhedral (See figure 43) and trimmed meshers (See figure42). They both give similar results but trimmed meshes require less memory than polyhedral meshes. As it is been said, both have been proven on this class of problem. Polyhedral have the advantage of smooth growth away from the body while trimmed meshes tend to be more efficient at placing cells in the refinement areas. Polyhedral meshes also work better when variations in free stream flow direction are analysed using the same mesh. Although if a single flow direction is present, a trimmed mesh will provide the most efficient approach to getting good results. Anyhow, trimmed mesher is chosen for this case (See figure 41).

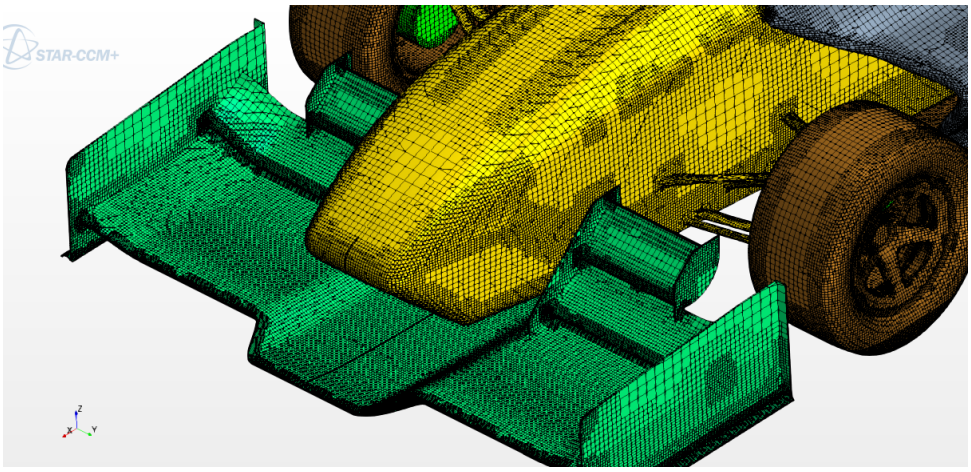

Figure 40. Volume Mesh detail of the front side of the car.

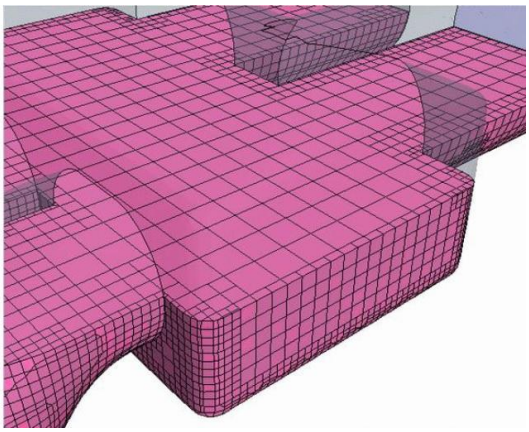

Figure 41. Trimmed mesh. (Source: Star CCM+ User Guide. Image by CD-ADAPCO)

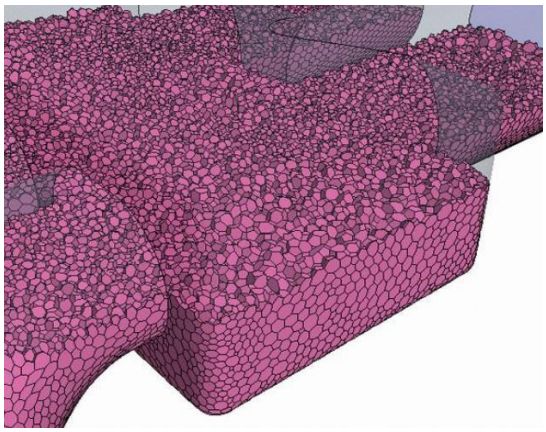

Figure 42. Polyhedral mesh. (Source: Star CCM+ User Guide. Image by CD-ADAPCO)

4.3.2. Capturing the ground effect with the mesh

The mesh is a key factor to capture the ground effect. Prism layers on the floor and in the underbody of the car have to be located. There must be enough prism layers to resolve the boundary layer accurately and also the transition between the prism layer mesh and the core mesh has to be the smoothest possible. The core mesh between the car and the ground has to be very refined and if it is possible with anisotropic cells. The growth of this anisotropic cells region in direction of the lift should be less than 10mm, depending on the ground clearance.
Regarding to physic and boundary condition settings, the floor has to be in movement if this is an open road simulation and wheels have to be rotating.

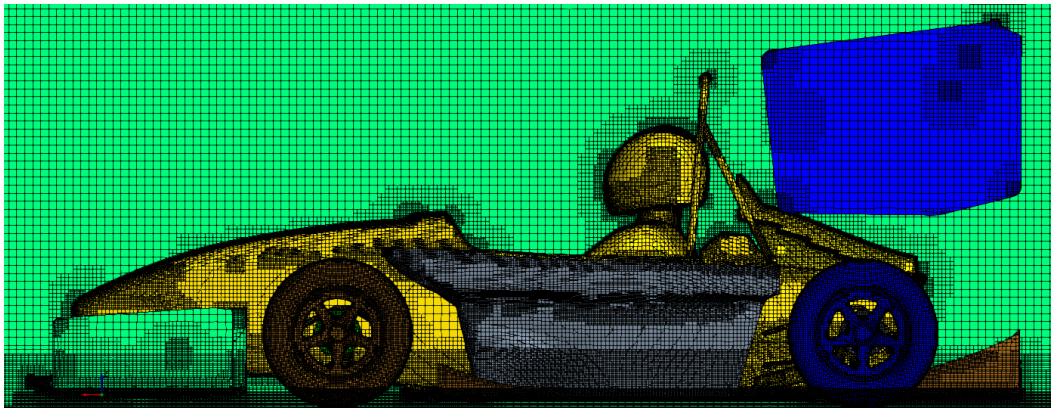

Figure 43. Volume mesh of the car.

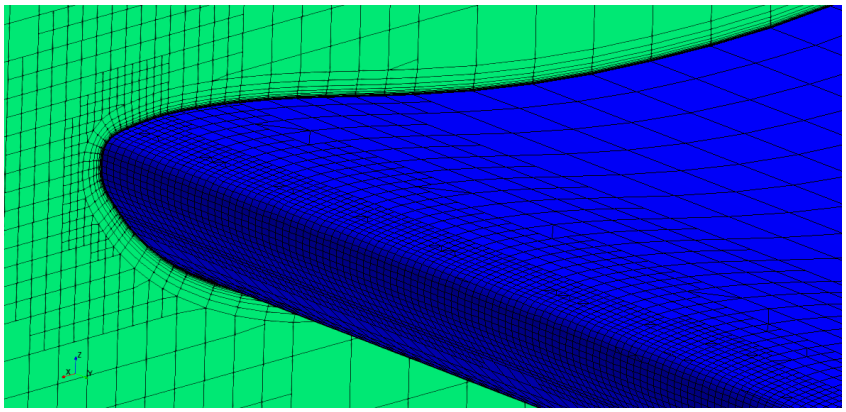

Figure 44. Detail of volume mesh around the mainplate of the rear wing .

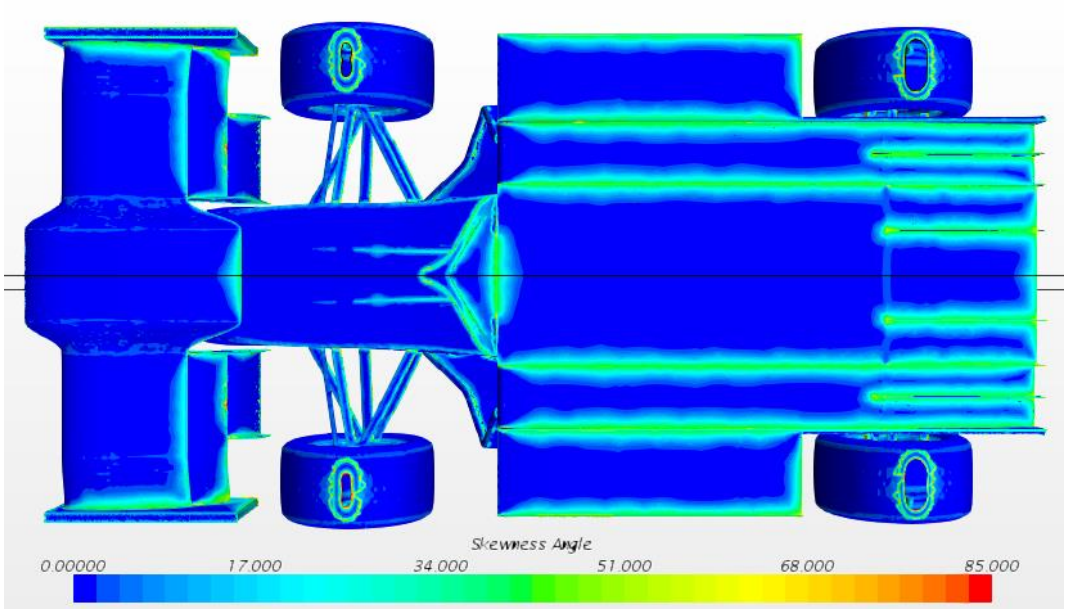

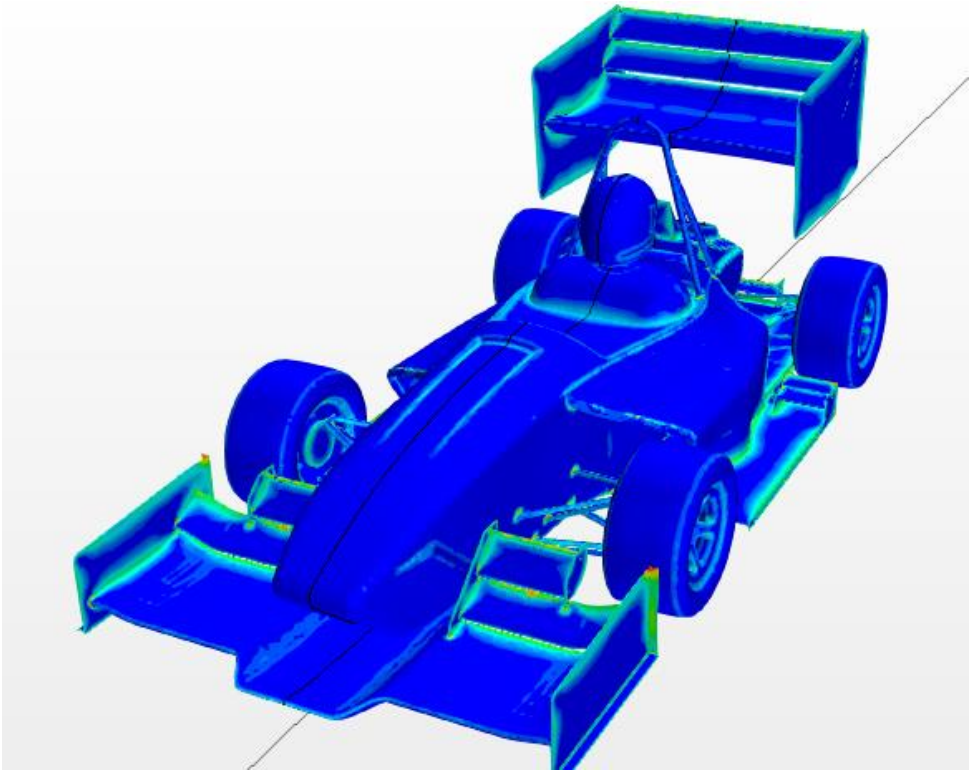

Figure 45. Scalar scenes of the skewness angle value over the car

Skewness is defined as the difference between the shape of the cell and the shape of an equilateral cell of equivalent volume. CD-ADAPCO recommends to have values lower than 85, so we can conclude that this is a good distribution (See figure 46).

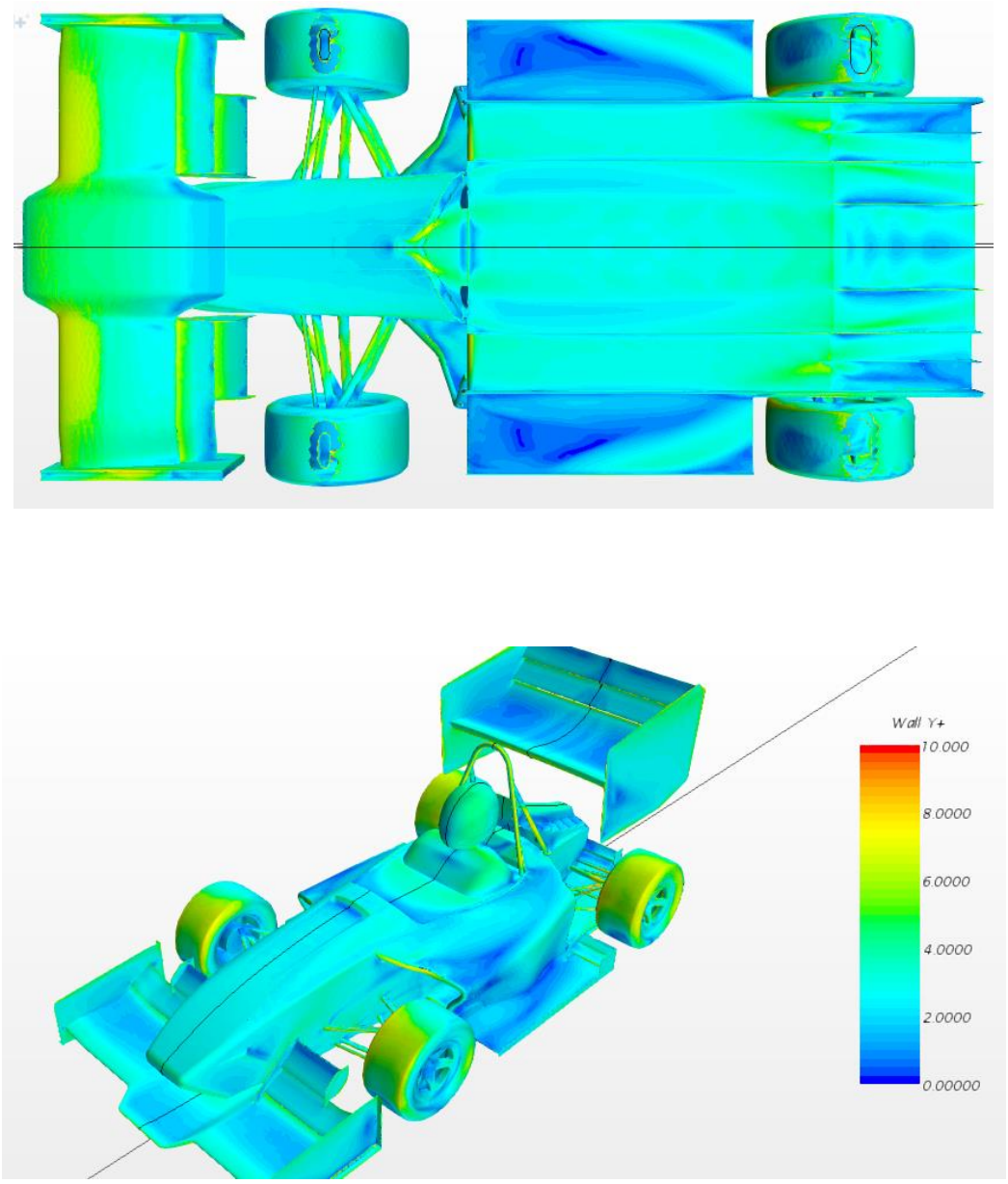

Figure 46. Wall Y+ values over the car.

As it can be seen on the pictures upon (figure 47), most of it has a Wall Y+ value lower than 5 which means that the viscous layer is solved quite well.

4.4. TURBULENCE TREATMENT

4.4.1. Turbulence Model

As the airflow around a race car is very turbulent, a model needs to be selected for the simulation of turbulent flow. Nowadays there are many turbulence models available to calculate the problems. The most common in the automotive industries are k-ε, k-ω, Lattice-Boltzmann and Large Eddy Simulation (LES). Of these models the k-ε and k-ω are most widely used with the k-ε said to be the most stable. Therefore, the Realizable k-ε turbulence model was selected based on other similar works [4] and also on CD-ADAPCO recommendations. Interesting information about turbulence models was found looking into the literature as [15]. However, the decision was made after trying some simulations with k-ω SST and seeing that the solution was not smooth and stable.

4.4.2. Wall treatment

See [13]] to further detail information about what is described next in this chapter.

Prism layer

In order to solve in the right way the near the wall effects, a prism layer mesh within the region next to the wall is needed. A prism layer mesh is a kind of mesh composed of prismatic cells whose growth is very smooth and goes from the wall to the core mesh or main mesh. These cells are supposed to simulate all the turbulent effects near the walls and its thickness and number of cells is determined by the turbulent model and near the wall treatment function used.

Law of the wall

To understand why a prism layer is needed and what happens in those layers, we have the law of the wall. The law of the wall is valid for high-Reynolds numbers and states that the average velocity of a turbulent flow at a certain point is proportional to the logarithm of the distance from that point to the wall (or the boundary of the fluid region). It is applicable to parts of the flow that are close to the wall (<20% of

the height of the flow). Therefore this is an indication of the required prism layer mesh resolution.

For this, we work with dimensionless velocity u+ and distance from the wall y+. The flow near a model surface can be largely subdivided into three regions (See figure 48).

The y^+ value is the dimensionless wall distance. It is the wall distance times the shear velocity divided the kinematic viscosity (see equations below).

$$y^+ = \frac{yu_\tau}{\upsilon}\ , u_\tau = \sqrt{\frac{\tau_w}{\rho}} \text{ and } u^+ = \frac{u}{u_\tau}$$

Where,

$y^+$is the wall coordinate

$u^+$is the dimensionless velocity

τ_w is the wall shear stress

ρ is the fluid density

u_τ is called the friction velocity or shear velocity

υ is the kinematic viscosity

In CFD y^+ is used in turbulence models that need the wall distance for modelling the influence of Reynolds stress tensor. Another use of y^+ is deducing the low-Reynolds and high-Reynolds models. The low-Reynolds model requires a first cell height so that the y^+ is less than one. On the other hand high-Reynolds models use wall functions and usually assume y^+ values at the first point above the wall to be at least one order of magnitude larger.

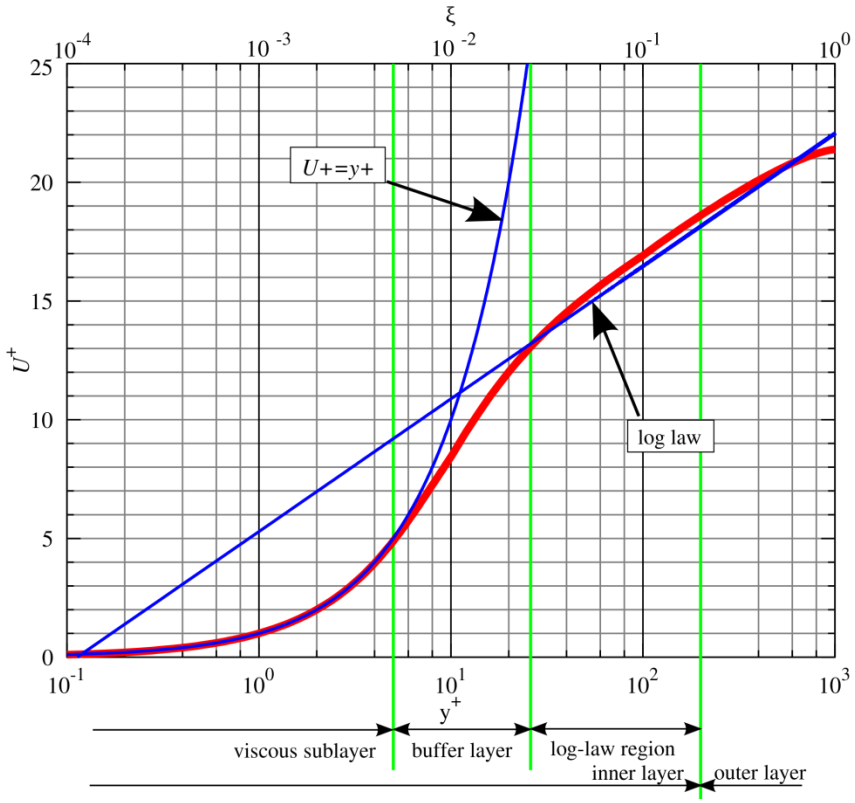

Figure 47. Law of the wall plot.

Viscous sublayer:

In this sublayer the flow is under viscous shear effect due to the fact that when the flow is very close to the model wall it is stationary and therefore it causes turbulence. The result of this is a turbulent shear stress within the extremely thin viscous sublayer when y+<5.

$$u^+ = y^+$$

Buffer layer:

Within this layer (5<y+<30), outside of the viscous sublayer the shear stress is assumed to be constant and equal to the wall shear stress. As far as the log-law layer is concerned we have:

$$u^+ = \frac{1}{k} y^+ + B = \frac{1}{k} lnEy^+$$

Where k, B and E are universal constants for turbulent flows that depend on the roughness of the wall. In case of a smooth wall k = 0.4, B = 5.5 and E = 9.8.

Outer layer:

Finally this layer is placed far away from the wall and viscous effects are negligible.

Wall functions

- **Near wall function (low y+)**

For this wall treatment the mesh resolution needs to be fine enough in order to resolve the viscous sublayer.

This wall treatment requires:

- y+ at the wall-adjacent cell should be around order of y+=1.
- As long as y+ at that cell doesn't exceed y+=5 is acceptable.
- At least 8-10 cells in that near wall region are required.

- **Wall functions (high y+)**

In this case, the viscous sublayer and buffer layer are not resolved, and thus the mesh resolution doesn't need to be as fine as the near wall treatment. By using this wall treatment method the required computational power is reduced. Y+ value must be higher than 30.

4.5. SETTINGS OF MESH AND BOUNDARY CONDITIONS

- **Open Road simulation:** The car moves forward while the air and ground have relative velocity to the car in opposite direction.
-
    - Boundary Conditions: Moving ground at the same velocity magnitude and direction as the air and modelled with No-Slip condition. Side and top walls => Slip walls.

- **Wind tunnel simulation:** Stationary simulation. No boundary layer because of the boundary layer suction devices, it means that Slip condition is set at the height where the suction devices are installed. Side walls and top walls => Slip walls.

To summarize:

Mesh Setting	Value
Mesh Type	Trimmer
Base size	24mm
Nº of Prism layers	8
Near wall thickness	0.1mm
Nº of volumetric controls	6
Below the car refinement size	10% of base size

Table 7. Mesh Settings.

Boundary	Condition
Ground	No-Slip. Moving ground equal to free stream
Top	Slip wall
Wall	Slip wall
Symmetry plane	Symmetry plane
Inlet	Velocity inlet. V= 20 m/s
Outlet	Pressure Outlet. P= 0 Pa
Car	No-Slip. Fixed
Wheels	No-Slip. Rotating wheels
Radiator	Porous region

Table 8. Boundary Conditions.

What is done in real F1 wind tunnels

In order to assure that the boundary conditions chosen are fine, below is a short explanation about the practices that Formula One teams do in wind tunnels to test the performance of their cars. See reference [8].

Teams in Formula 1 as the very first motorsport reference all over the world, have very complex and expensive wind tunnels which are designed for simulating almost every detail that the car can experiment on the track. These wind tunnels have moving ground technology, they can remove the boundary layer on the ground using suction devices, they can also simulate yaw movements and some of them have adaptive walls to correct the blockage effect.

Focusing on “Boundary condition at the ground”, an important difference between what happens in a wind tunnel and when the car drives over the track is the generated boundary layer on the ground. This is given because when any flow has friction to a stationary surface, a growth of the boundary layer occurs. It grows all along the section of the tunnel and then there is no peak of air velocity on the ground. That is why on recirculating wind tunnels there are sections of contraction to decrease the boundary layer as much as possible besides the present suction devices in the working section which are specially thought for that function.

For that reason, in wind tunnel testing there is technology needed to avoid and remove the boundary layer, because on the race track “it doesn’t really exist” if you ignore the wind and its atmospheric boundary layer.

The common technology for this is suction patches with holes in it in front of the working section to remove the air and accelerate the first layers near the surface.

In wind tunnels the ground is moving synchronized to the air speed and it generates the rotation of the wheels as well. Once atmospheric air on Surface is removed and a moving ground is synchronized to the air speed, it is supposed that there won’t be boundary layer growth.

4.6. DESIGN OF THE UNDERTRAY

4.6.1. Optimization concept

The chosen criterion of the optimization of the diffuser, and thus getting the most efficient diffuser was the aerodynamic efficiency (Lift/Drag). Variations were done only changing the diffuser angle relative to the ground. This was the only varied aspect because the geometry of the design was already fixed as straight conduct. So the main goal was to get the angle which produced less flow separation leading also to less drag. In order to find out what would be the best design for an undertray, the aerodynamic efficiency of the diffuser has been parametrized as a function of the angle relative to the ground. The table below shows the maximum efficiency reached for this diffuser.

Boundary and physics conditions of this test

Velocity of the free stream v = 20m/s, Re = $5.1 \cdot 10^5$. Also air density used for the calculations is $\rho = 1.18415$ kg/m^3 and dynamic viscosity $\mu = 1.85508 \cdot 10^{-5}$ Pa·s.

To calculate the coefficients only the top of the diffuser has been taken as lifting body. The height of the constraint section is 4cm according to the ground clearance of the car and the boundary condition at the ground is no-slip with relative tangential velocity equal to the free stream velocity. The computational domain goes further the real outlet of the diffuser, see figure 48. See figure 49 for the detailed view of the cross section at the diffuser region.

See table 9 for boundary conditions of the computational domain and table 10 for the results

Boundary	Condition
Inlet	Velocity Inlet (free stream Velocity)
Outlet	Pressure Outlet (0Pa)
Top	No-Slip. Fixed velocity v=0
Wall*	No-Slip. Fixed velocity v=0
Ground	No Slip Condition – Moving ground. Same speed of the free stream

Table 9. Boundary conditions for the diffuser optimization case. See figure 48.

*This wall is built upon the diffuser outlet in order to simulate and see the influences of the fluid domain after the diffuser (See figure 48).

Computational domain of the diffuser study and results

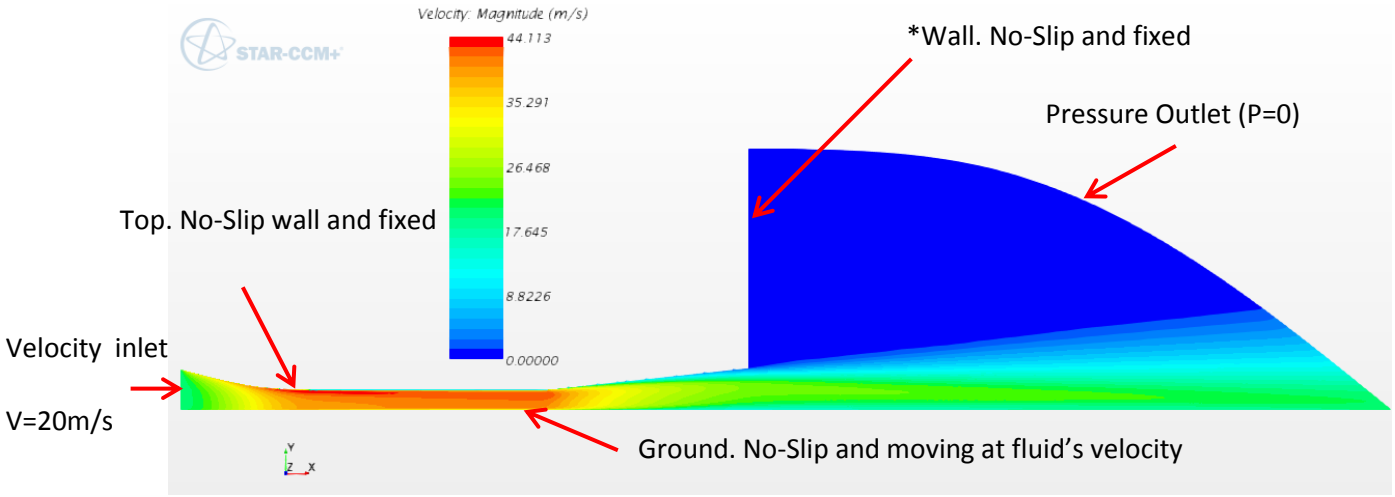

Figure 48. Computational domain for the simulations of the diffuser. The represented field function is velocity.

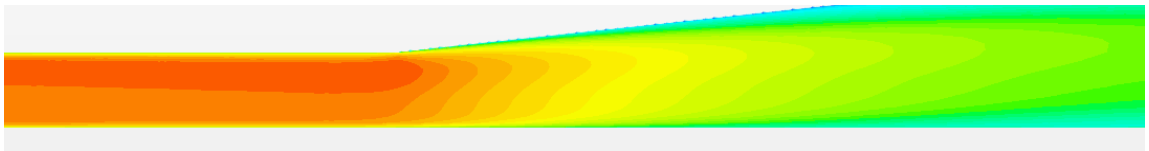

Figure 49. Cross section detail of the diffuser's 2D velocity field with 6º angle relative to the ground. It has been the most efficient

Angle (º)	CL	CD	CL/CD
15º	-0,904	0,061	-14,713
12º	-1,394	0,040	-34,860
11º	-1,477	0,037	-39,397
10º	-1,589	0,035	-46,028
9º	-1,675	0,033	-51,456
8º	-1,747	0,031	-56,012
7º	-1,782	0,030	-58,864
6º	-1,762	0,030	-59,340
5º	-1,676	0,030	-55,794
4º	-1,548	0,031	-50,253

Table 10. Diffuser efficiency given by ration CL/CD as a function of the angle of the diffuser to the ground. Re = 5.1·105.

4.7. FULL VEHICLE SIMULATIONS

In order to see the improvement on the downforce made by the undertray, different simulations of the car have been undertaken. First of all, the entire car without aeropackage has been tested and afterwards the entire car with different variations of the undertray. The cell count is over 7 million in every case and always half model using a symmetry plane. The results of the simulation for the following cases are shown in the table below. Velocity inlet is 20m/s and yaw angle is 0 deg. These results are of the half model, so Lift and Drag must be multiplied by 2. Force coefficients CL and CD remain constant for both cases due to their definition. All the values have been properly rounded to 2 decimals of precision. Negative lift values mean downforce. See table 11 for results.

Test	CL	CD	Lift (N)	Drag (N)	Lift/Drag
Without Aeropackage	0.28	0.53	24.11	45.19	0.53
Without Undertray	-2.54	1.21	303.6	145.26	2.10
With Undertray	-2.78	1.23	331.545	146.67	2.26

Table 11. Aerodynamic performance of the half car.

From the results in the table it is very clear that the undertray has a very important role for the performance of the entire car. The car itself without aerodynamic devices generates positive lift. By adding the front and rear wings this drastically

changes and the car gets negative values of lift, so the downforce is a fact. We can see that the drag of the car without any aerodynamic element is the 30% of the total drag after adding front and rear wings. Almost the same drag generates the car with the undertray. This high value of drag is given because of the open wheel design of a formula style car and also due to the big wings set on the car. Rotating wheels are important lift generators because at the point where the tyres are in contact with the ground, there is stagnation pressure (zero velocity). Assuming the results for the full car as the ones in table 9 multiplied per 2:

Test	Lift overall (N)	Drag overall (N)	Downforce generated (N)
Without Aeropackage	48.22	90.38	-
Without Undertray	607.19	290.51	660.35
With Undertray	-663.09	293.33	679.22

Table 12. Aerodynamic performance of the full car.

In the column downforce generated there is only the value of the downforce generated by wings and undertray. Lift overall is the value for the full car with all its parts, same for drag overall.

Analysis of Lift and Drag by parts

Without aeropackage

Lift overall (N)	Drag overall (N)	Downforce generated (N)
48.22	90.38	-

Table 13. Aerodynamic overall performance of the car without aeropackage.

Part	Downforce (N)	Drag (N)
Monocoque	-29.64	45.69
Wheels	-18.58	44.69

Table 14. Aerodynamic performance of the car without aeropackage by parts.

No downforce is generated at all because the car itself generates lift. It is very clear that aerodynamic elements to generate downward pressure are needed.

Without Undertray

Lift overall (N)	Drag overall (N)	Downforce generated (N)
607.19	290.514	660.35

Table 15. Aerodynamic overall performance of the car without undertray.

Part	Downforce (N)	Drag (N)
Front Wing	334.83	48.92
Rear Wing	325.52	120.6
Monocoque	-30.78	73.26
Wheels	-22.38	47.734

Table 16. Aerodynamic performance of the car without undertray by parts.

Full aeropackage

Lift overall (N)	Drag overall (N)	Downforce generated (N)
-663.09	293.33	679.22

Table 17. Aerodynamic overall performance of the full car.

Part	Downforce (N)	Drag (N)
Front Wing	333.38	48.18
Rear Wing	316.55	119.89
Monocoque + Undertray	29.29	75.79
Wheels	-16.13	49.47

Table 18. Lift and Drag of the full car by parts.

Part	Downforce (N)	Drag (N)
Undertray itself*	60.07	2.53

Table 19. Theoretical undertray's aerodynamic performance.

It can be seen in table 18 that including the undertray to the monocoque changes the value lift from positive to negative (downforce) by 60.07N. It also increases the drag by 2.53N. Therefore we can say that the undertray is the most efficient aerodynamic device of the car although the results are not as good as could be.

4.7.1 Results discussion

Unfortunately, the downforce generated by the aerodynamic elements is not the definitive overall lift value. This is because the formula style car and the rotating uncovered wheels that are positive lift generators. Anyhow the rest of the car is able to generate huge amounts of downforce, enough to depreciate the positive values of the monocoque and tyres. For the case without undertray, it has improved from +48.22N to -607.19N, so the total real downforce generated is only reduced in 8% (from 660.35N to 607.19n) due to the monocoque and tyres (See tables 13 and 15).

The influence of the undertray to the drag is practically inexistent increasing the drag coefficient in only 2 hundredth from 1.21 to 1.23 (See table 11). On the other hand lift is affected by the diffuser and it increases the aerodynamic performance. With the undertray the overall downforce increases by 8.4% while the drag less than 1%. Regarding only to the undertray, any existent positive lift of the bodywork is made disappear (See table 18). The lift generated all over the monocoque and wheels is positive and around 50N in each test (over 40% of this only by the wheels). When the undertray is part of the bottom of the monocoque it has no positive lift anymore.

Just looking to the overall downforce, including the undertray it improves as said before around 8.4% of the overall performance, which doesn't seem to be so much. However it is a part stack to the monocoque which is a positive lift generator.

Flow around the car

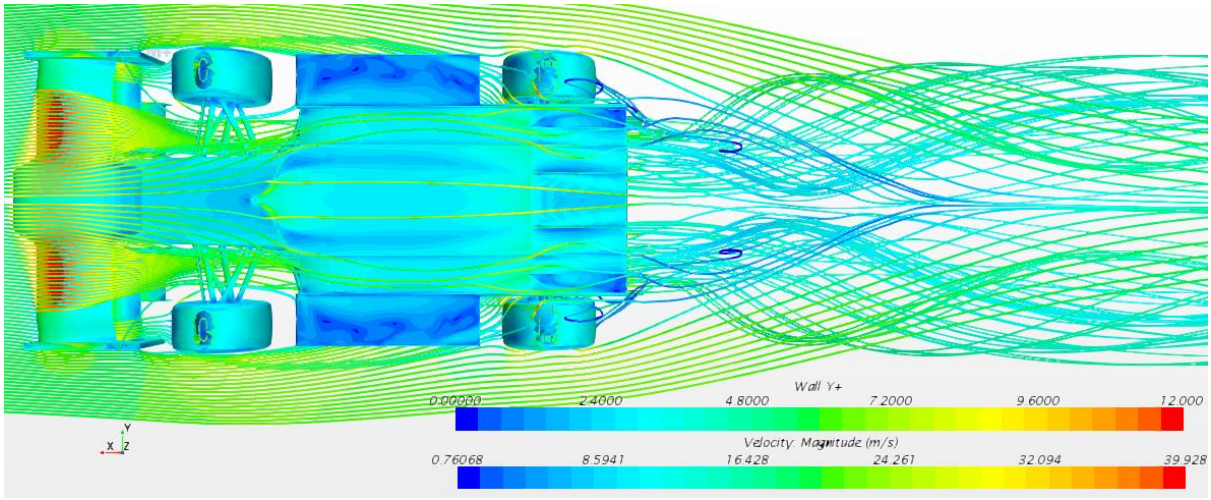

Figure 50. Streamlines underneath. Wall Y+ on the car surface. Velocity magnitude for the streamlines.

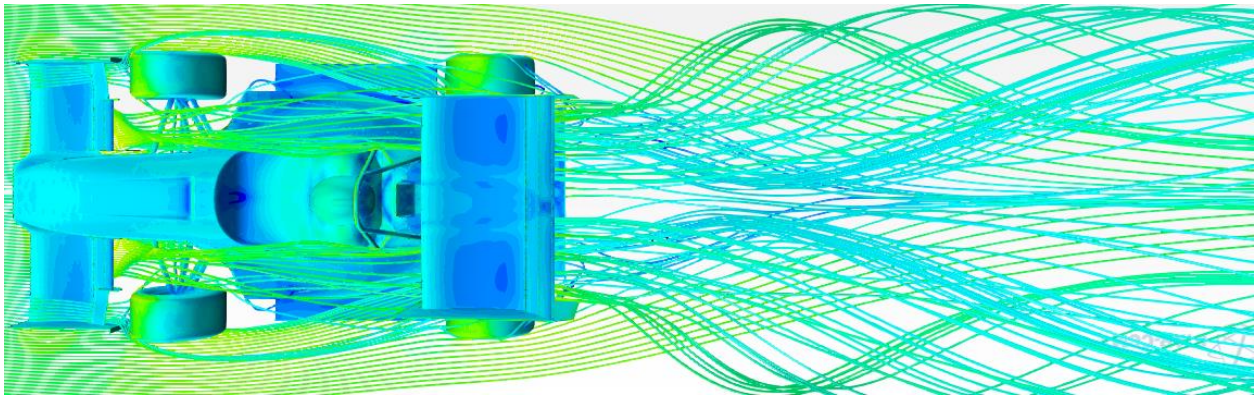

Figure 51. Opposite view to figure 50.

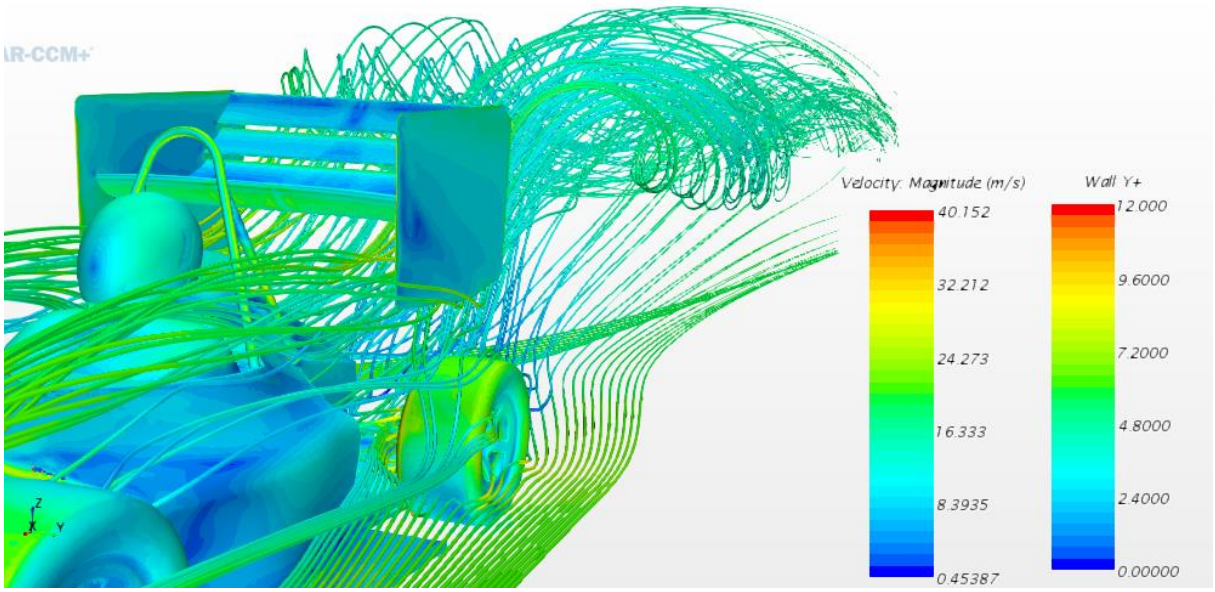

Figure 52. Detail of the streamlines behind the car. Wake area and vortices are generated.

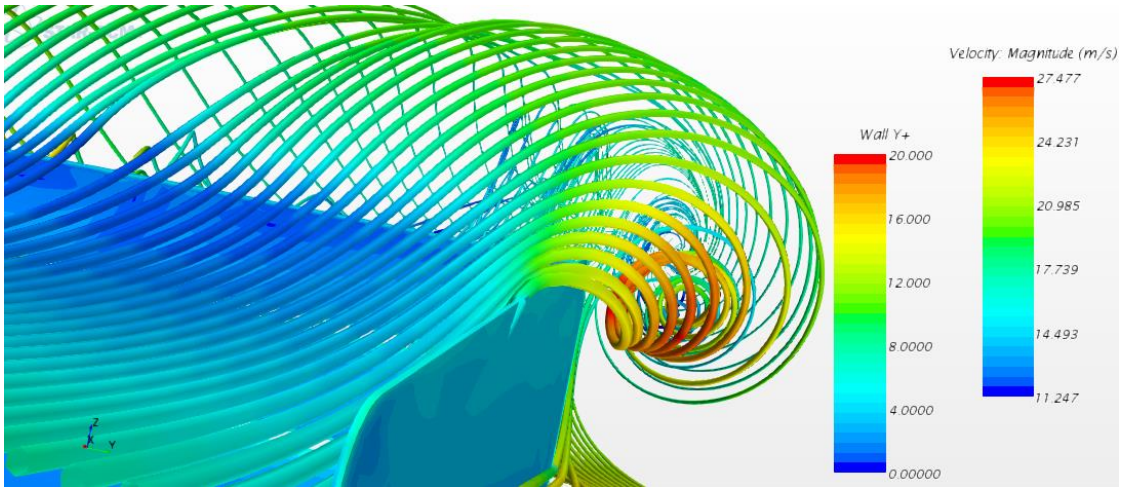

Figure 53. Rear wing vortices detail.

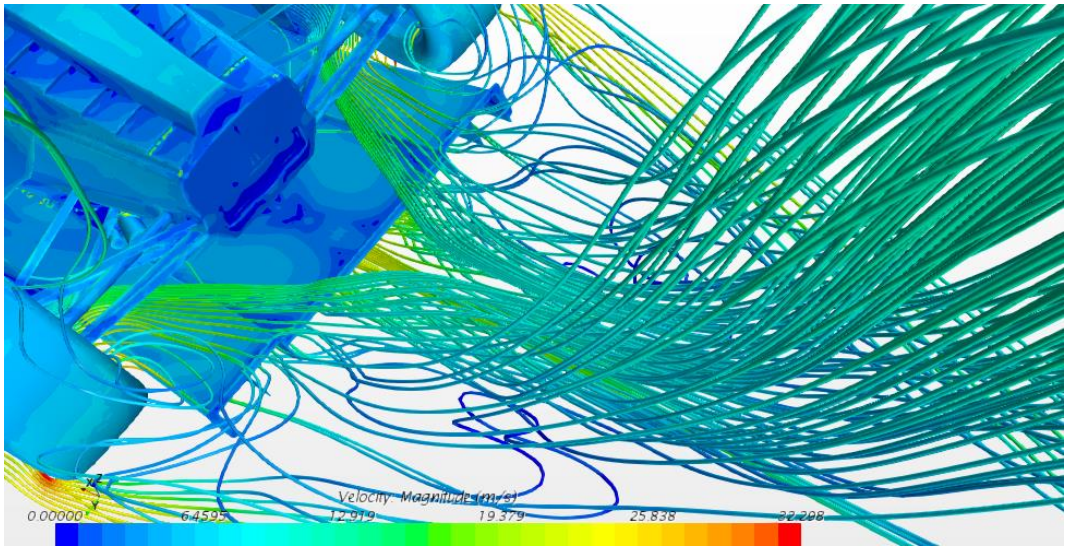

Figure 54. Flow behind the diffuser.

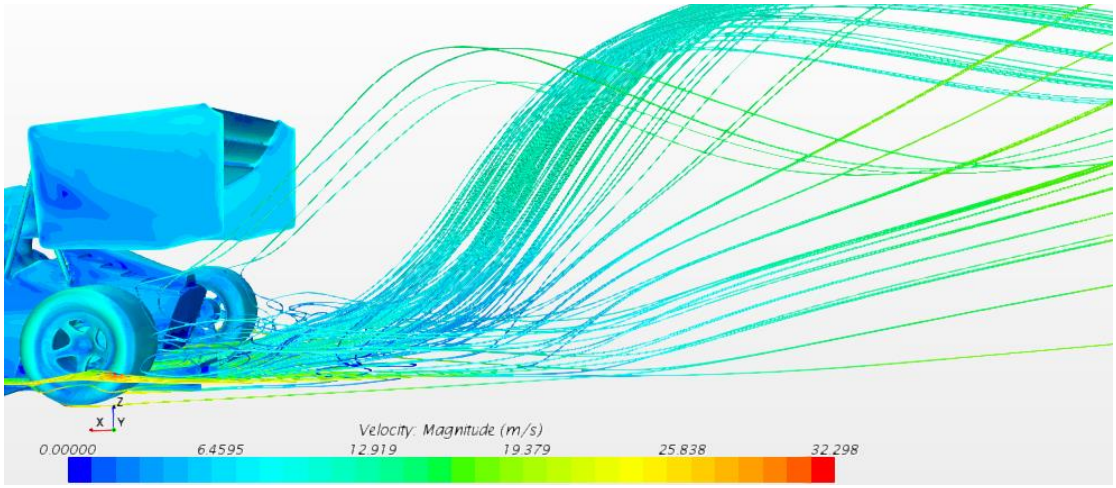

Figure 55. Wake produced by the outcoming flow of the diffuser.

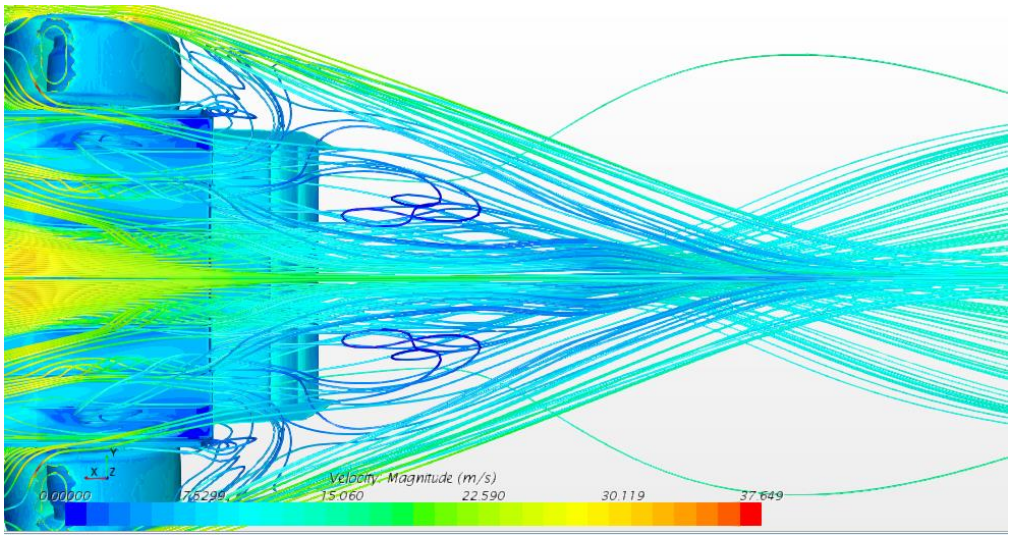

Figure 56. Detail of streamlines underneath the car at the diffuser region.

Taking a look at figures from 50 to 56, it is proved that a race car is aerodynamically a succession of connected vortices all around the car surface. Dealing well with them will allow the car have better stability and aerodynamic performance. After the wings a vortex is created which increases drag. Endplates are used to weak these vortex but don't remove them.

Another thing that can be seen clearly is that all the flow underneath tend to exit by the centre of the car. Thus the airflow through lateral conducts of the undertray changes its direction at the end of the car and exits by the central diffuser. This is bad because half of the design is not working and a lot of possible downforce amount is lost here. Right after the diffuser the wake starts and huge vortices appear.

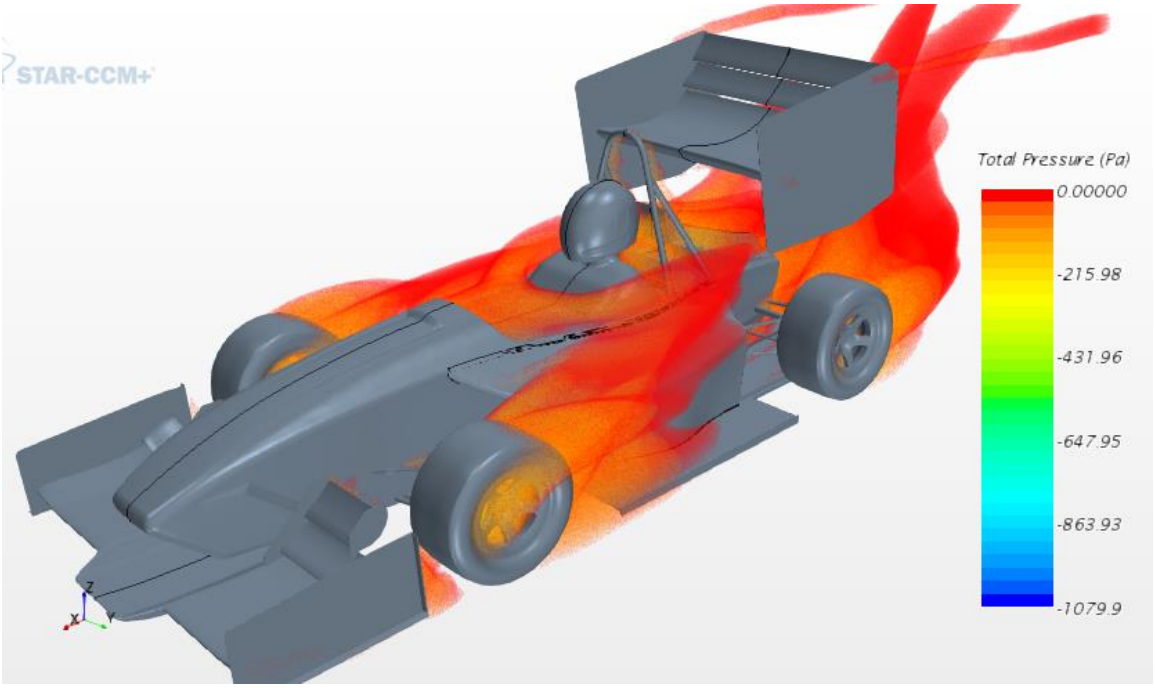

Figure 57. Volumetric view of the total pressure around the car.

By setting the maximum pressure representation at 0Pa, it allows seeing the wake around the car. The front wheels generates a big wake and also behind the car which is expected. Total pressure is the sum of the static pressure plus the dynamic pressure and the gravitational. If there is no height variation, then only static and dynamics pressures are considered.

Pressure distribution over the car surface

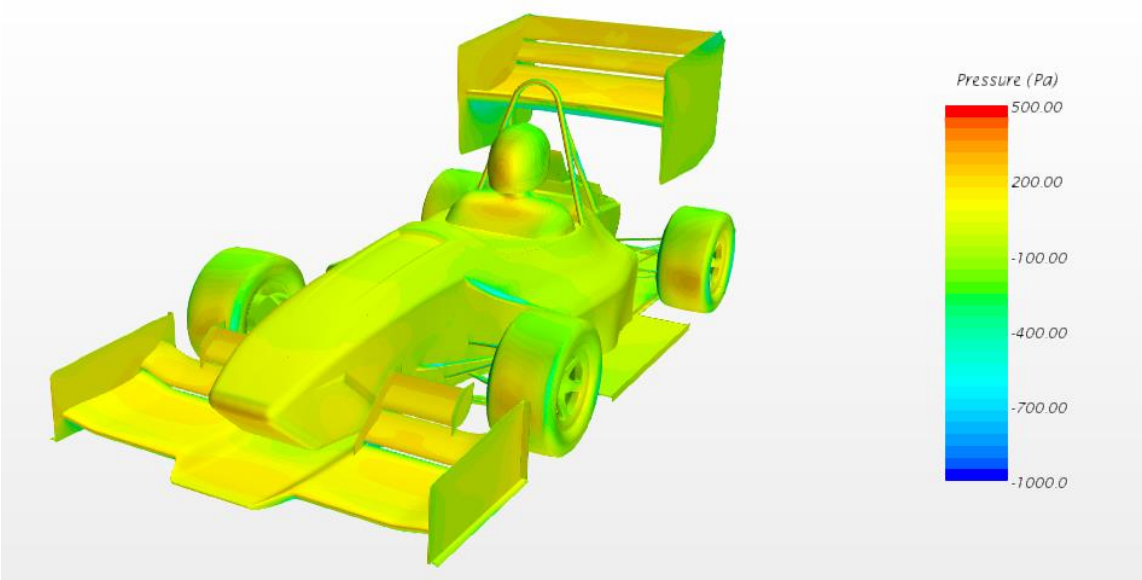

Figure 58. Pressure distribution of the whole car.

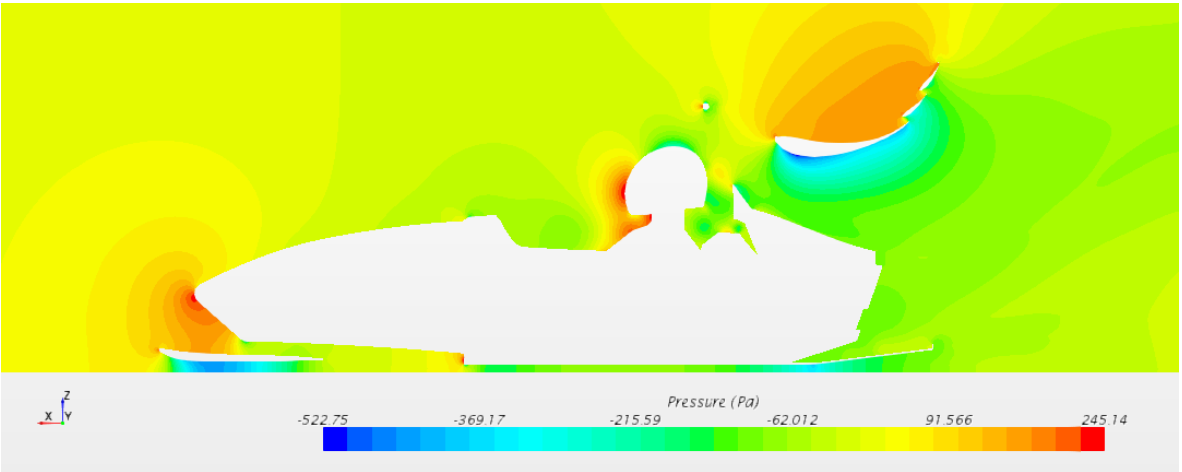

Figure 59. Scalar field around the car by its symmetry plane.

Pressure distribution by parts

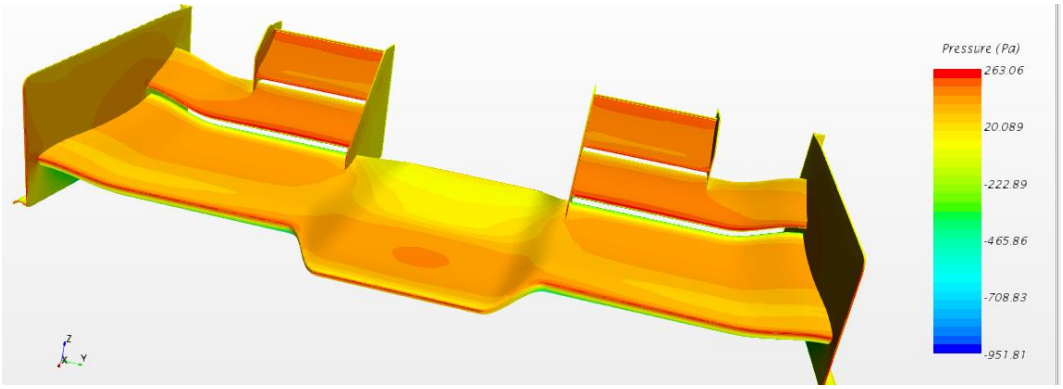

Figure 60. Frontal view of the front wing.

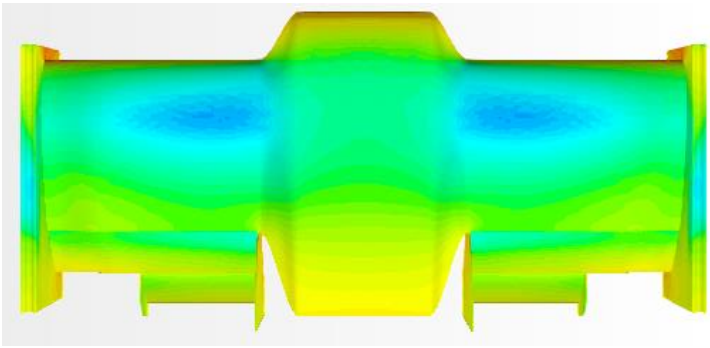

Figure 61. Front wing viewed from down side. Upper side in the picture is the front. See figure 52 for the colour bar.

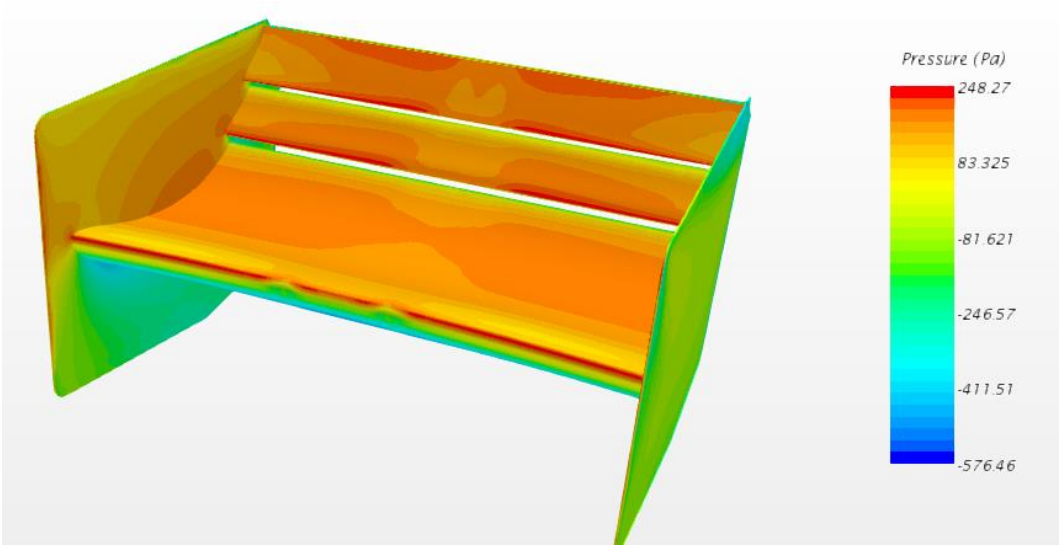

Figure 62. Rear wing in general view.

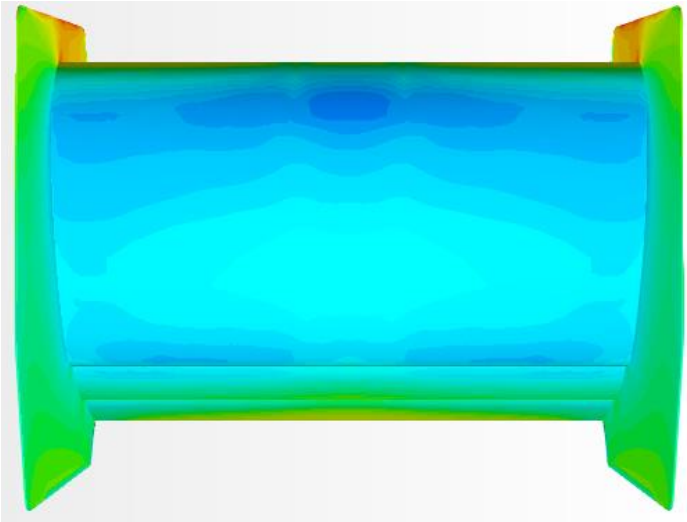

Figure 63. Rear wing from down side. See figure 54 for the colour bar.

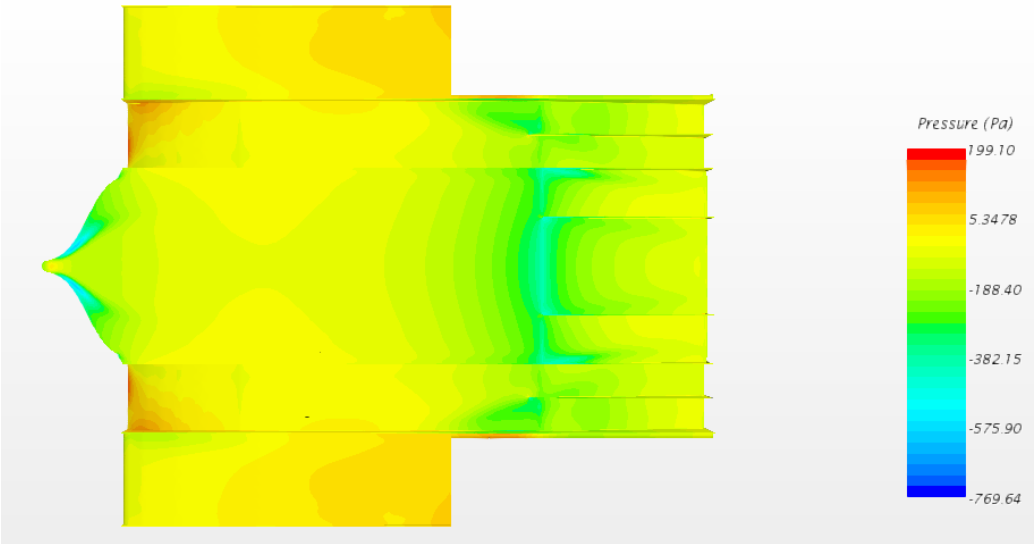

Figure 64. Pressure distribution of the undertray.

4.7.2. Final undertray design

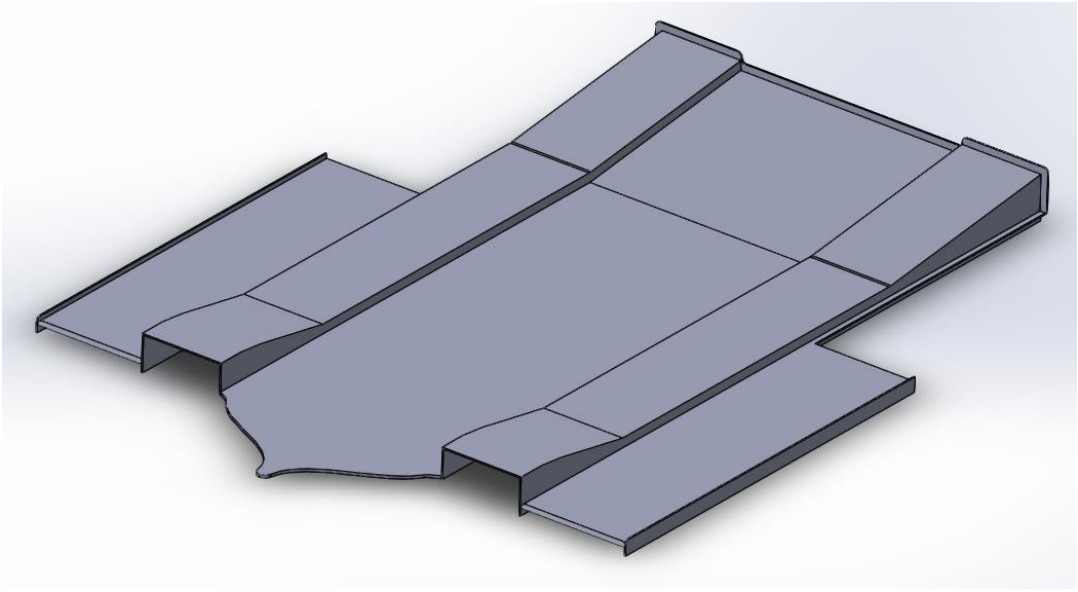

Figure 65. Final Design of the Undertray

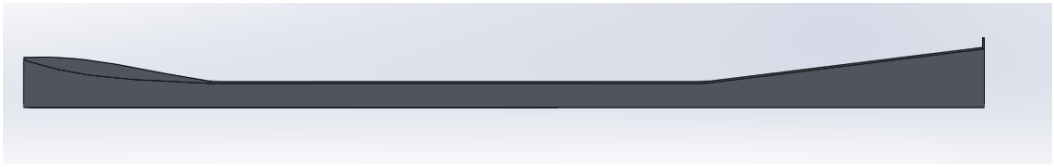

Figure 66. Cross section of the lateral conduct of the undertray. Inlet on the left side.

4.7.3 Other tested designs

Due to the low improvement made by the undertray itself, some other designs with the willing of giving some extra aid to generate downforce were designed.

- One version of the undertray with a back wing upon the central region of the diffuser was tested just to try to generate a low pressure area above the diffuser to reduce flow separation at the exit. However this did not produce good results.

- When small lateral wings where added just in front of the back wheels downforce did not increase significantly either. The problem was still there, the lateral conducts of the undertray which are located right down the sidepods don't work as they are supposed to, and thus not enough low

pressure is generated. The point is to try to find a solution to make more clean air pass through them.

- Taking a look at the streamlines around the car, another version of the undertray but this time with lateral inlets where the streamlines were supposed to go was designed and tested. Again, this design was not successful but this was expected, because more air was injected to where the air was supposed to be extracted from.

- Also a diffuser with larger angles was tested because and again, it did not work well.

5. CONCLUSIONS

Throughout this work it can be seen that aerodynamic elements can really improve the performance of a racing car in terms of its stability on high speed corners increasing the downward pressure onto the car and top speeds on straights reducing the drag. Although the results for the undertray have not been as good as expected, they still show the importance of this element and the advantage that can be achieved on track even at low speeds if the complete aerodynamic design works fine together. Anyway the car with the undertray is more stable than without it and allows having more traction through the corners.

Design results aside, it can be said that an important goal of this work that was very time demanding has been successfully achieved. It is the good CFD configuration even using Star CCM+ on a conventional laptop instead of on a high performance computer. A fine mesh with more than 7 million cells, good near the wall treatment and accurate convergence of the residuals that make the results trustable, can be managed on a personal laptop.

6. BIBLIOGRAPHY

[1] W. F. Milliken and D. L. Milliken, Race Car Vehicle Dynamics, Society of Automotive Engineers Inc. USA, 1995

[2] Dr. H. Schlichting, Chapter XXI, Turbulent boundary layers, flat plate. In Boundary-Layer theory, McGraw-Hill, USA, 1979

[3] Simon McBeath, Aerodinámica del automóvil de competición, Ed. CEAC, 2005

[4] R. Carrese and H. Winarto, "Parametric study of airfoil proximity to the ground", (paper, Royal Melbourne Institute of Technology, n.d.)

[5] N. R. Kapania and K. Terracciano and S. Taylor, "Modelling the fluid flow around airfoils using conformal mapping" (paper, 2008)

[6] Nor Elyana Ahmadi and Essam Abo-Serie and Adrian Gaylard, "Mesh optimization for ground vehicle aerodynamics" (journal, Coventry University, UK, Vol. 2(1) – March 2010)

[7] K. Jensen, Aerodynamic Undertray Design for Formula SAE, Master Thesis, Oregon State University, 2010

[8] W. Toet, How wind tunnels work – F1 Explained – Sauber F1 Team [Online] Available: www.youtube.com/watch?v=KC0E0wU6inU

[9] [Online] Available: www.formula1-dictionary.net

[10] CD-ADAPCO, Star CCM+ User Guide [Online] Available: http://stevedocs.cd-adapco.com

[11] CD-ADAPCO, FSAE Technical Resource Guide [Online] Available: https://steve.cd-adapco.com/articles/en_US/FAQ/FSAE-Technical-Resource-Guide

[12] J. Katz and A. Plotkin, Low-Speed Aerodynamics, Cambridge Univ. Press, 2001.

[13] J. Bredberg, "On the Wall Boundary Condition for Turbulence Models", (internal report, Chalmers University of Technology, 2000.)

[14] J. D. Anderson Jr., Fundamentals of Aerodynamics, McGraw-Hill, third edition, USA, 2001

[15] R.A.W.M. Henkes, Overview of Turbulence Models for External Aerodynamics, Delft University Press, 1998

[16] D. Matos Chaves, Implementation of a 2D Panel Method for Potential Flow Past Multi-Element Airfoil Configurations, Technical University of Lisbon, 2012

[17] Stephen B. Pope, Turbulent Flows, Cambridge University Press, October 2000

[18] P. Niedermeyer, Automotive History: An Illustrated History of Automotive Aerodynamics, [Online] Available: http://www.curbsideclassic.com/automotive-histories/automotive-history-an-illustrated-history-of-automotive-aerodynamics-part-1-1899-1939/, January 26, 2012

[19] R. Temam, Navier-Stokes Equations theory and numerical analysis, North-Holland Publishing Company, 1977

[20] CAR The definitive visual history of the automobile (Dorling Kindersley Editor), 2011